





DUDLEY KNOX LIBRARY  
NAVAL POSTGRADUATE SCHOOL  
MONTEREY, CALIFORNIA 93943-5002



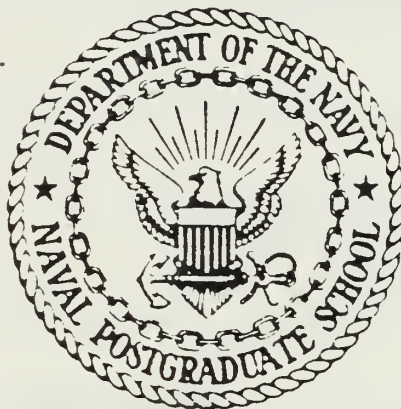






# NAVAL POSTGRADUATE SCHOOL

Monterey, California



## THESIS

HOT CORROSION BEHAVIOR OF MODIFIED ALUMINIDE  
COATINGS ON COBALT-BASE SUPERALLOYS

by

Muhammad Yasin

June 1986

Thesis Advisor:

D. H. Boone

Approved for public release; distribution is unlimited.

T233062





## REPORT DOCUMENTATION PAGE

REPORT SECURITY CLASSIFICATION		1b. RESTRICTIVE MARKINGS	
SECURITY CLASSIFICATION AUTHORITY		3 DISTRIBUTION/AVAILABILITY OF REPORT	
DECLASSIFICATION/DOWNGRADING SCHEDULE		Approved for public release; distribution is unlimited.	
PERFORMING ORGANIZATION REPORT NUMBER(S)		5 MONITORING ORGANIZATION REPORT NUMBER(S)	
NAME OF PERFORMING ORGANIZATION		6b OFFICE SYMBOL (If applicable)	
Naval Postgraduate School		Code 69	
7a. NAME OF MONITORING ORGANIZATION		7b. ADDRESS (City, State, and ZIP Code)	
Naval Postgraduate School		Monterey, CA 93943-5100	
NAME OF FUNDING/SPONSORING ORGANIZATION		8b OFFICE SYMBOL (If applicable)	
ADDRESS (City, State, and ZIP Code)		9 PROCUREMENT INSTRUMENT IDENTIFICATION NUMBER	
ADDRESS (City, State, and ZIP Code)		10 SOURCE OF FUNDING NUMBERS	
		PROGRAM ELEMENT NO	
		PROJECT NO	
		TASK NO	
		WORK UNIT ACCESSION NO	
TITLE (Include Security Classification)			
T CORROSION BEHAVIOR OF MODIFIED ALUMINIDE COATINGS ON COBALT-BASE SUPERALLOYS			
PERSONAL AUTHOR(S)			
asin, Muhammad			
TYPE OF REPORT		13b TIME COVERED	
Master's Thesis		FROM _____ TO _____	
14 DATE OF REPORT (Year, Month, Day)		15 PAGE COUNT	
1986 June		86	
SUPPLEMENTARY NOTATION			
COSATI CODES		18 SUBJECT TERMS (Continue on reverse if necessary and identify by block number)	
FIELD	GROUP	SUB-GROUP	
		Modified Aluminide Coatings, Cobalt-Base Superalloys	
ABSTRACT (Continue on reverse if necessary and identify by block number)			
Marine gas turbines experience a number of detrimental operating conditions as a result of environment and fuel variation. There are two types of hot corrosion which occur in marine and other types of gas turbines known as low temperature hot corrosion and high temperature hot corrosion. Protective coatings are necessary and have been widely used to improve hot corrosion resistance for superalloys operating in this environment. Considerable data can be obtained from the literature on systems applied			
DISTRIBUTION/AVAILABILITY OF ABSTRACT		21 ABSTRACT SECURITY CLASSIFICATION	
<input checked="" type="checkbox"/> UNCLASSIFIED/UNLIMITED <input type="checkbox"/> SAME AS RPT <input type="checkbox"/> DTIC USERS		Unclassified	
NAME OF RESPONSIBLE INDIVIDUAL		22b TELEPHONE (Include Area Code)	
Donald H. Boone		(408) 646-2656	
		22c OFFICE SYMBOL	
		Code 69B1	

to nickel-base superalloys while little data are available on similarly coated cobalt-base superalloys. This study was initiated to evaluate the behavior of modified coatings on a series of cobalt-base superalloys in both high and low temperature hot corrosion.

Approved for public release; distribution is unlimited.

Hot Corrosion Behavior of Modified Aluminide  
Coatings on Cobalt-Base Superalloys

by

Muhammad Yasin  
Lieutenant Commander, Indonesian Navy  
B.S., Naval Academy, 1970  
M.E., Naval Institute of Science, 1979

Submitted in partial fulfillment of the  
requirements for the degree of

MASTER OF SCIENCE IN MECHANICAL ENGINEERING

from the

NAVAL POSTGRADUATE SCHOOL  
June 1986

245  
6.1

## ABSTRACT

Marine gas turbines experience a number of detrimental operating conditions as a result of environment and fuel variation. There are two types of hot corrosion which occur in marine and other types of gas turbines known as low temperature hot corrosion and high temperature hot corrosion. Protective coatings are necessary and have been widely used to improve hot corrosion resistance for superalloys operating in this environment. Considerable data can be obtained from the literature on systems applied to nickel-base superalloys while little data are available on similarly coated cobalt-base superalloys. This study was initiated to evaluate the behavior of modified coatings on a series of cobalt-base superalloys in both high and low temperature hot corrosion.

## TABLE OF CONTENTS

I.	INTRODUCTION . . . . .	12
A.	MARINE GAS TURBINE . . . . .	12
B.	HOT CORROSION . . . . .	13
C.	COATINGS . . . . .	14
D.	MODIFIED-ALUMINIDE COATINGS. . . . .	23
	1. Platinum modified-aluminide coatings. . . . .	23
	2. Chromium modified aluminide coating. . . . .	25
	3. Platinum-Chromium modified aluminide coatings. . . . .	27
II.	EXPERIMENTAL PROCEDURE . . . . .	29
A.	BACKGROUND . . . . .	29
B.	HOT CORROSION TESTING . . . . .	32
III.	RESULTS AND DISCUSSION . . . . .	35
A.	HOT CORROSION RESISTANCE OF VARIOUS COATINGS ON MAR-M-509 SUBSTRATE. . . . .	35
B.	HOT CORROSION RESISTANCE OF VARIOUS COATINGS ON X-40 SUBSTRATE. . . . .	37
C.	HOT CORROSION RESISTANCE OF VARIOUS COATINGS ON FSX-414 SUBSTRATE. . . . .	38
D.	HOT CORROSION RESISTANCE OF VARIOUS COATINGS ON WI-52 SUBSTRATE. . . . .	40
E.	HOT CORROSION RESISTANCE OF EB-PVD COBALT CHROMIUM ALUMINUM YTTRIUM AND PLATINUM-ALUMINIDE COATINGS ON IN-738 AS CONTROL SAMPLE. . . . .	40



F.	STANDARD ALUMINIDE COATING ON VARIOUS SUPERALLOYS. . . . .	41
G.	PLATINUM ALUMINIDE COATING ON VARIOUS SUPERALLOYS. . . . .	42
H.	PLATINUM CHROMIUM ALUMINIDE COATING ON VARIOUS SUPERALLOYS. . . . .	43
I.	RHODIUM-ALUMINIDE COATING ON MAR-M-509 AND WI-52 SUBSTRATES. . . . .	44
J.	RHODIUM-PLATINUM-ALUMINIDE COATING ON MAR-M-509 AND FSX-414 SUBSTRATES. . . . .	44
IV.	CONCLUSIONS AND RECOMMENDATIONS . . . . .	47
APPENDIX A:	TABLE I-V . . . . .	49
APPENDIX B:	FIGURE B.1-B.25 . . . . .	55
LIST OF REFERENCES	. . . . .	80
INITIAL DISTRIBUTION LIST	. . . . .	86

## LIST OF TABLES

I	MECHANISMS OF HOT CORROSION . . . . .	49
II	LIST OF SPECIMENS . . . . .	51
III	NOMINAL COMPOSITION (WT.%) OF CAST SUPERALLOYS . . . . .	52
IV	COATING MANUFACTURING PROCESS . . . . .	53
V	RESULTS OF HOT CORROSION DATA . . . . .	54

## LIST OF FIGURES

B.1	Relative rates of attack . . . . .	55
B.2	Graphical representation of hot corrosion data at 900 and 700 C . . . . .	56
B.3	High and low temperature hot corrosion behavior of various coatings on MAR-M-509 substrate . . . . .	57
B.4	High and low temperature hot corrosion behavior of various coatings on X-40 substrate . . . . .	58
B.5	High and low temperature hot corrosion behavior of various coatings on FSX-414 substrate . . . . .	59
B.6	High and low temperature hot corrosion behavior of various coatings on WI-52 and IN-738 substrates . . . . .	60
B.7	Effects of Std-Al coatings on various superalloys . . . . .	61
B.8	Effects of Pt-Al coatings on various superalloys . . . . .	62
B.9	Effects of Pt-Cr-Al coatings on various superalloys . . . . .	63
B.10	Effects of Rh-Al coatings on MAR-M-509 and WI-52 substrates . . . . .	64
B.11	Effects of Rh-Pt-Al coatings on MAR-M-509 and FSX-414 substrates . . . . .	65
B.12	SEM photomicrographs of Std-Al coatings on MAR-M-509 substrate: (a) exposed 200 hrs at 900 C, (b) exposed 60 hrs at 700 C and (c) as-received . . . . .	66
B.13	SEM photomicrographs of Pt-Al coatings on MAR-M-509 substrate: (a) exposed 200 hrs at 900 C, (b) exposed 60 hrs at 700 C and (c) as-received . . . . .	67

B. 14	SEM photomicrographs of Pt-Cr-Al coatings on MAR-M-509 substrate: (a) exposed 200 hrs at 900 C, (b) exposed 60 hrs at 700 C and (c) as-received . . . . .	68
B. 15	SEM photomicrographs of CVD-Low Al coatings on MAR-M-509 substrate: (a) exposed 200 hrs at 900 C, (b) exposed 60 hrs at 700 C and (c) as-received . . . . .	69
B. 16	SEM photomicrographs : (a) Rh-Al coatings and (b) Rh-Pt-Al coatings on MAR-M-509 substrate both exposed 200 hrs at 900 C . . . . .	70
B. 17	SEM photomicrographs of Std-Al coatings on X-40 substrate: (a) exposed 200 hrs at 900 C, (b) exposed 60 hrs at 700 C and (c) as-received . . . . .	71
B. 18	SEM photomicrographs of Pt-Al coatings on X-40 substrate: (a) exposed 200 hrs at 900 C, (b) exposed 60 hrs at 700 C and (c) as-received . . . . .	72
B. 19	SEM photomicrographs of Pt-Cr-Al coatings on X-40 substrate: (a) exposed 200 hrs at 900 C, (b) exposed 60 hrs at 700 C and (c) as-received . . . . .	73
B. 20	SEM photomicrographs of Std-Al coatings on FSX-414 substrate: (a) exposed 200 hrs at 900 C, (b) exposed 60 hrs at 700 C and (c) as-received . . . . .	74
B. 21	SEM photomicrographs of Pt-Al coatings on FSX-414 substrate: (a) exposed 200 hrs at 900 C, (b) exposed 60 hrs at 700 C and (c) as-received . . . . .	75
B. 22	SEM photomicrographs of Pt-Cr-Al coatings on FSX-414 substrate: (a) exposed 200 hrs at 900 C, (b) exposed 60 hrs at 700 C and (c) as-received . . . . .	76
B. 23	SEM photomicrographs of Rh-Pt-Al coatings on FSX-414 substrate exposed 200 hrs at 900 C . . . . .	77
B. 24	SEM photomicrographs: (a) aluminide pack process coating and (b) Rh-Al coating on WI-52 substrate both exposed 200 hrs at 900 C . . . . .	78

B.25 SEM photomicrographs: (a) EB-PVD CoCrAlY coating exposed 200 hrs at 900 C, (b) and (c) Pt-Al coatings both exposed 200 hrs at 900 C and 60 hrs at 700 C, respectively . . . . . 79



## ACKNOWLEDGEMENT

First of all, I have to thank God ( ALLAH SWT.) for giving me life to go through all the experiences in the world, particularly, in the world of science and technology. Secondly, my gratitude goes to the United States Government which has given me the opportunity to study at the Naval Postgraduate School.

I also wish to extend my heartfelt gratitude to Dr. D.H. Boone who has given his valuable time in guiding me and providing the necessary pointers in completing this thesis.

I extend my deepest appreciation to Dr. Prabir Deb for his guidance and cooperation and thereby making my work lighter and able to be completed on time. Special thanks goes to Tammy Bloomer and Tom Kellogg for their assistance and cooperation.

For coating production and heat treatment I extend my appreciation to Dr. S. Shankar of the Turbine Components Corporation and to Mr. J.S. Smith and C. Thomas of Howmet Corporation.

For my beloved wife, Rafnila, and children, Ali Utama, Benyamin, and Zuleika who have been patient and resolute in facing the separation of almost three years and have given me great moral support. To them I dedicate all I have done.

## I. INTRODUCTION

### A. MARINE GAS TURBINE

Gas turbines have been accepted as the most powerful engines being used in both aircraft and ships. Some of the advantages that gas turbines offer as a marine propulsion engines include features such as compact installation, rapid start from cold conditions, high performance, high reliability, simple maintenance, and minimum smoke generation [Ref. 1].

One problem encountered in the gas turbines is hot corrosion associated with the elevated temperatures experienced, particularly on the first turbine airfoils. Many studies have been performed to identify the causes and to establish the best way to solve these problems. The development of marine gas turbines propulsion systems in the United States, particularly in the U.S. Navy, was initiated in the 1960's with the GTS.Callaghan, the first ship outfitted with the gas turbine engines as the propulsion source. From the observation onboard the GTS.Callaghan it was found unexpectedly that turbine component degradation was more severe in the low temperature region than at the higher temperatures, the first time this was recognized by the Navy.

## B. HOT CORROSION

Gas turbines operating in industrial environments compared to gas turbines used in the marine environment, last up to five times longer. The life limiting components are the first stage blades and vanes whose failure is caused by hot corrosion attack resulting in large part from the contaminants in the fuel and the ingested air. Hot corrosion attack is an aggressive attack of hot gas path components resulting from the combined effects of normal oxidation plus reaction with the inlet air and fuel contaminant [Ref. 2]. Gas turbine hot corrosion attack is now recognized to be caused by molten sodium sulfate and related compound condensed on the blade surface and sulfur oxides in the gas.. The sodium sulfate can dissolve the protective oxides which results in rapid substrate attack and eventually the formation of internal sulfides. Temperature, frequency of thermal cycling, and the use of water washing are factors that affect the aggressiveness of hot corrosion attack.

There are two types of hot corrosion which are known to occur in gas turbine engines. They are known as low temperature hot corrosion (LTHC) and high temperature hot corrosion (HTHC). Low temperature hot corrosion is a very aggressive attack which occurs at metal temperatures of approximately 600-750 C. High temperature hot corrosion

attack occurs at metal temperatures of approximately 800-1000 C. Low temperature hot corrosion attack is characterized by no depletion of the aluminum and other alloying element zone ahead of the corrosion interface while high temperature hot corrosion attack is characterized by the depletion of elements from the coating and subsequent oxidation attack of the denuded zone. Corrosion rates under the low temperature hot corrosion condition are often greater than at the high temperature hot corrosion condition.

### C. COATINGS

The development of superalloys with sufficient creep and tensile strength at temperatures required for the economic use of a gas turbine has resulted in materials with insufficient surface stability for satisfactory life. Surface coatings are found to be the most effective method of solving the major problems encountered by gas turbines in the marine environments. Some coatings have good high temperature hot corrosion resistance but are less effective in low temperature hot corrosion environments, while others are good in low temperature hot corrosion resistance and essentially non-protective in high temperature hot corrosion conditions. Hence, it is important to first understand the mechanisms of hot corrosion degradation for the development of suitable protective coatings. Investigation on the two types of hot corrosion has revealed that hot corrosion

attack exhibits two stages [Ref. 3: p. 666]. The first stage is initiation where the alloys behave as if they do not have any deposit. The second stage is that of corrosion propagation where the alloys have a deposit which renders the protective properties of the oxide scales non-existent.

During the initiation stage process the surface of the alloy is being degraded at a rate similar to the superalloys surface in the absence of deposit. From this point of view it is clear that the surface should be maintained in the initiation stage as long as possible. In marine environments it is not possible to have such conditions occur because of the extremely harsh conditions experienced. Therefore, most systems exhibit a very short initiation stage. The nature of the initiation stage process is still not fully understood [Ref. 4]. During the initiation stage, the deposits start to attack the surface by oxidation. Chromium and aluminum diffuse to react with oxygen to form internal oxide layers below the outer surface. The composition of these oxide layers depends on the composition of the alloy. With chromium or aluminum present the internal oxide layers will form a protective barrier and will be supplied by further elemental diffusion from the substrate. This first stage will come to an end when the chromium and aluminum have been sufficiently depleted and the oxide barrier is penetrated. The initiation stage process rate



depends on such factors as alloy composition, alloy surface conditions, gas environment, and the occurrence of cracking of the oxide scales [Ref. 5: p. 14].

The second stage of attack is propagation, which results in the component being removed, the propagation stage always has much larger corrosion rates than the initiation stage. During the propagation stage the degradation of the alloy is taking place. As stated earlier, the nature of the initiation stage process is still not fully understood but much more data are available on the propagation stage of hot corrosion. In the marine environment the formation of the deposits on the blades and vanes of gas turbines results in a condition which causes a reaction with the substrate.

Superalloys such as IN-738 consist of elements that have high affinities for oxygen which will create an oxygen gradient across the deposit. It is apparent that the effect of the deposit is to separate the superalloy from the gas environment and produce a lower oxygen activity over the alloy surface. This condition then leads to the activities of other reactants in the gas increasing and causes selective oxide formation to be difficult in the presence of a deposit. Initially, an oxide barrier will form but thermally induced stresses will damage the scales and less protective oxides will form with foreign deposits on the surface. In addition, the protective oxide scales which are

formed may dissolve in the deposits and create another undesirable conditions known as a fluxing reaction of the protective oxide barrier [Refs. 6,7].

The salt fluxing reactions on superalloys can be either basic or acidic depending on the composition of the alloy and the gaseous environment. In IN-738 the propagation stage can be either basic fluxing, sulfidation, or acidic fluxing [Refs. 8,9]. By removing sulfur from sodium sulfate, a basic fluxing reaction will occur and produce oxide ions which react with the protective oxide scale. The amount and type of deposit on the surface of the superalloy determine the concentration of oxide ions for basic fluxing. Basic fluxing reactions require a source of sodium sulfate in order for this kind of degradation to continuously occur.

The acidic fluxing reaction is different from the basic fluxing reaction. It involves the development of non-protective reaction products on the surface in which the deposit (sodium sulfate) has a deficiency of oxide ions. This phenomena occurs when an acidic component is present in the gas or an acidic phase is formed as an oxidation product of the alloy [Refs. 10,11,12]. Then there are two types of acidic fluxing, that is to say, alloy induced acidic fluxing and gas phase induced acidic fluxing. The presence of acidic components such as sulfur trioxide in the gas causes the non-protective oxide scale to form as a result of the

high diffusion velocity of certain ionic species in the acidic melt [Refs. 10,11,12]. The acidic melt causes the attack to become self-sustaining even with only a small amount of sodium sulfate present [Ref. 7]. Molybdenum, vanadium, and tungsten as refractory metal elements will form oxide and cause the sodium sulfate to become acidic. These elements when oxidized as a result of the deposit (sodium sulfate) on an alloy can cause catastrophic self-sustaining hot corrosion through acidic fluxing.

Sulfur and chlorine are elements in superalloy deposits that can also cause a non-protective oxide scale to be formed. Sulfur induced degradation is the primary case of hot corrosion of superalloys in gas turbines. Chloride ions in the deposit which cause oxide scales such as alumina and chromia will be more susceptible to cracking and spalling [Ref. 13].

Basic fluxing, alloy induced acidic fluxing, sulfur and chlorine induced degradation normally become significant in the high temperature hot corrosion range (800-1000 C). While gas phase induced acidic fluxing becomes significant in the low temperature hot corrosion range (600-700 C). The pressure of sulfur trioxide in the gas phase decreases as temperature is increased. The presence of sulfur trioxide in the gas phase can cause the sodium sulfate deposit to become liquid at temperatures as low as 600 C.

Figure B.1 shows the temperature range over which the different hot corrosion propagation modes are most significant [Ref. 3]. Table I lists a summary of the hot corrosion mechanisms [Ref. 3].

Protective coatings for gas turbine superalloy airfoils should be resistant to: thermal cyclic oxidation, hot corrosion, and thermal fatigue cracking. Other factors such as an effect on airfoil creep behavior, an effect on high frequency fatigue resistance, and resistance to particulate erosion should be considered for practical applications [Ref. 14]. There are essentially three types of protective coatings used in high temperature turbine operation, the diffusion, overlay, and thermal barrier systems [Ref. 15].

Diffusion coatings use two primary methods for processing, the slurry-fusion and pack cementation techniques with the latter being most widely used. In the slurry fusion process, an aluminum alloy is sprayed or dipped onto the substrate to a certain thickness and then the system is heat treated at a temperature of about 870-1090 C to produce diffusional formation of the coating. The pack cementation process is a form of chemical vapor deposition and the structural types are dependent on the vapor aluminum activity [Refs. 16,17]. In the pack cementation process the articles are embedded in a powder mixture of aluminum alloy, an ammonium hallide as an activator, and

alumina as an inert diluent. The 'pack' is heated in the temperature range from 650 to 1090 C for times ranging from two to twenty-four hours. Subsequent heat treatment should be accomplished in order to further diffuse the coating and develop the proper mechanical properties of the superalloy. The resulting structures are governed primarily by the nature of the diffusional formation of two principle intermetallic compounds in the nickel-aluminum system [Ref. 17].

A considerable amount of works has been done to investigate the mode of degradation of these diffusion coatings. Processes such as cyclic oxidation, hot corrosion, interdiffusion, erosion, and mechanical effects are various combinations that contribute to coatings degradation [Ref. 14]. The effects of a diffusion aluminide coating on high frequency fatigue behavior have been observed on Udimet-700, where at room temperature to 480 C the coating increases the fatigue strength. Above 480 C the fatigue strength decreases up to about 700 C at which point no influence is observed [Ref. 18].

Diffusion aluminide coatings have two archetypical coating structures on nickel-base superalloys classified as inward and outward. Inward type coatings are formed by conducting the process of diffusion aluminizing in high activity, aluminum rich packs, at low temperatures from 700



to 950 C. Outward type coatings are formed by conducting the process of aluminizing in low activity, aluminum lean packs, at high temperatures, ranging from 1000 to 1100 C. Both types are followed by a post coating diffusion heat treatment (generally 1080 C / 4 hours). These two archetypical coatings are known as low temperature high activity (LTHA) and high temperature low activity (HTLA) [Ref. 17].

Overlay coatings were developed in order to solve the problems encountered with diffusion coatings. Overlay coatings can be fabricated by foil claddings, plasma spray, and electron beam evaporation or sputtering techniques. Higher interdiffusion does not occur which allows the structure and composition of the overlay coatings to be varied essentially independent of the substrate. Hot corrosion resistance and ductility can be increased without significantly degrading the substrate's mechanical properties. These coatings have non-interactive properties which allow for the variation of chemical composition to match substrate properties and service requirements. However, the overlay coatings do not solve all the problems. Higher cost because of complex application techniques and quality control have often limited their use [Ref. 19].

MCrAlY coatings (M=Fe, Ni, Co, and/or combination thereof) are the genesis overlay coatings type which are applied by either physical vapor deposition, as typified by

sputtering and electron beam evaporation, or advanced plasma spray techniques [Refs. 26,27,28]. The first series of MCrAlY coatings was FeCrAlY [Ref. 29]. This FeCrAlY coating is applied to nickel-base superalloys and exhibits an increase in durability compare to diffusion aluminide coatings, particularly in high temperature hot corrosion resistance. However, the formation of NiAl at the interface of FeCrAlY and substrate causes a loss of aluminum and becomes life limiting [Ref. 14: p. 806]. A series of more diffusionally stable coatings have been developed such as CoCrAlY [Ref. 30], NiCrAlY [Ref. 31], and NiCoCrAlY [Ref. 32].

Thermal barrier coatings based on stabilized zirconium oxide are used to improve the durability of sheet metal components in gas turbines where the idea is to insulate the metals from the thermal effects of high temperature gaseous attack [Ref. 20]. These coatings have at least two layer, which are usually applied by plasma spray techniques. Then consist of a layer of an oxidation resistant alloy and a stabilized zirconia layer overcoat. Gradation of metal through the metal-zirconia mixture to pure zirconia have been suggested to minimize the effects of thermal expansion mismatch stresses between zirconia and the substrate [Ref. 21]. The problem encountered in thermal barrier coating use on gas turbine airfoils is the thermal stress induced spallation of the insulating ceramic layer. The

application of ceramic thermal barrier coatings on marine gas turbines could be compromised by the presence of corrosive molten salts [Refs. 22,23,24]. Much work has been done in this area which has led to the conclusion that these coatings still show considerable promise for life extension of gas turbine components in clean fuel environments. Development work is being done for application in gas turbines using low grade fuels [Ref. 25].

#### D. MODIFIED-ALUMINIDE COATINGS.

##### 1. Platinum modified-aluminide coatings.

Noble metals ( platinum, rhodium, and palladium ) have been used to modified aluminide coatings for a numbers of years. Extensive studies have been performed in this area particularly on the platinum modified aluminide coating at the Naval Postgraduate School [Refs. 5,19,33,34].

The first commercial Pt-Al system which has since been improved, designated LDC-2, is reported to have a four-fold life in cyclic oxidation and greater than two-fold life in hot corrosion resistance improvement compare to an unmodified aluminide coatings [Ref. 35]. This was followed by a second commercial coating 'RT-22' produced by essentially the same process, electroplating platinum followed by a pack aluminizing treatment, which exhibits a different microstructure and platinum distribution. LDC-2 has a single phase  $PtAl_2$  surface structure while RT-22 has a two phase

structure. Investigation of these two commercial Pt-Al systems found that the oxidation behavior is dependent on the structure, i.e. the platinum distribution and phases present in the coatings [Ref. 36].

Platinum modified aluminide coatings, like the diffusion aluminide coatings, also have inward (LTHA) and outward (HTHA) structures which can affect their protectivity [Ref. 34: pp. 11-19]. The LTHA process in Pt-Al coatings is found to be less sensitive to surface attack at 900 C than the HTLA process. However, Pt-Al coatings with either the LTHA or HTLA process, have improved the hot corrosion resistance by at least a factor of six times compared to unmodified aluminide coatings with the same process [Ref. 37].

Hot corrosion behavior of platinum modified aluminide coatings on IN-738 substrates exhibit only limited beneficial effects at low temperature (700 C) compare to high temperature (900 C) [Refs. 37,38]. Pt-Al coatings inhibit the basic fluxing mechanisms of HTHC thereby increasing the hot corrosion resistance. The presence of Pt however does not inhibit the gas phase induced acidic fluxing mechanisms of LTHC which make it little better than an unmodified aluminide coating in hot corrosion resistance [Ref. 39].

The effects of surface structure under cyclic oxidation at 1100 C of platinum modified aluminide and unmodified aluminide coatings have also been investigated [Ref. 33]. From these studies it was found that the so called rumpling, the surface plastic instability, appears more in the platinum modified aluminide than in unmodified aluminide coatings. The thicker coatings on IN-738 superalloy substrate exhibit a lower propensity to rumple than the thinner coatings. However, cracking in the coating is found on thicker coating while no such case occur on thinner coating.

There are some data available on the mechanical properties of the platinum modified aluminide coatings. The investigation on ductile to brittle transition temperature (DBTT) behavior of the Pt-Al coatings has found that the DBTT is strongly structural dependent [Ref. 19]. The presence of platinum, at comparable aluminum levels, increases the DBTT and the room temperature residual compressive stress level. However, DBTT and residual stress can be varied by changing the composition and structure of the coatings.

## 2. Chromium modified aluminide coating.

One of the first modifying elements added to the aluminide coatings was chromium. Chromium has beneficial effects on hot corrosion resistance at low temperature by promoting the formation chromium oxide as a protective



barrier. However, at high temperature chromium oxide does not provide good HTHC resistance because it can volatilize to chromium trioxide at temperature above 800 C. However, chromium does contribute to HTHC resistance by decreasing the amount of aluminum required to form aluminum oxide in nickel-aluminum systems [Ref. 40].

Work on chromium modified aluminide coatings such as on the IN-738 and IN-100 superalloy substrates have found that these coatings have a three zone structure with LTHA processing [Ref. 5]. The surface zone has a high chromium content with a NiAl matrix and an alpha chromium precipitate because of the very low solubility of chromium in NiAl. The intermediate zone is a single phase NiAl and the innermost is the interdiffusion zone with chromium and other substrate refractory metal carbides in a NiAl matrix [Ref. 41].

The microstructures of these two superalloys substrates given the HTLA process show a large amount of chromium at the surface with the chromium precipitated in a NiAl matrix. It is found that concentration of chromium is higher near the interdiffusion zone than near the surface zone [Ref. 5]. Chromium modified aluminide coatings produced by the HTLA process show a characteristic microstructure that can be attributed to only outward type diffusion structures. In general, platinum modified aluminide and chromium modified aluminide coatings exhibit classic

microstructures associated with LTHA process, the inward aluminum diffusion, and HTLA process, the outward nickel diffusion, in the unmodified aluminide coatings [Ref. 42,43].

### 3. Platinum-Chromium modified aluminide coatings.

In a manner similar to the process found for the diffusion aluminide coatings, platinum plus chromium modified aluminide coatings also have inward and outward types of structures. However, by adding the two modified elements to an aluminide coating, this type of coating structure will become more complex. The chromium platinum modified aluminide coating has been investigated [Ref. 5]. One significant difference between these two kinds of coatings is the result of the order in which the modified elements are applied. Platinum chromium modified aluminide coatings have the coating elements applied in the order : 1) platinum, 2) chromium and 3) aluminum. While chromium platinum modified aluminide coatings have the coating elements applied in the order : 1) chromium, 2) platinum and 3) aluminum. Chromium platinum modified aluminide coatings exhibit a good low temperature hot corrosion resistance because of a high PtAl<sub>2</sub> layer at the surface zone with little Ni or Cr, while platinum chromium modified aluminide coating exhibit relatively poor resistance to LTHC attack which little PtAl<sub>2</sub> layer at the surface zone which contain a high Ni (NiAl) and some

chromium. It is clear that for these two types of coatings the dominant factor is PtAl<sub>2</sub> content at the surface layer as a barrier for LTHC resistance since both of them have a high chromium concentration level near the surface. By adding chromium as the first element and then platinum prior to the aluminizing process the result is PtAl<sub>2</sub> forming at the surface. Adding platinum first and then chromium before aluminizing causes the dispersion of the platinum in the intermediate zone. The structure of these two kinds of coatings obviously depend on the first modifying element to be applied [Ref. 34: p. 22]. These two kinds of coatings have been referred to as process B (Pt-Cr-Al) and process D (Cr-Pt-Al) [Refs. 5,34,43].

It is evident that the modified aluminide coatings offer good hot corrosion resistance compared to unmodified aluminide coatings. The dominant factor in their function as a barrier for hot corrosion resistance is a single phase PtAl<sub>2</sub> at the surface zone.

Most of the published studies of these modified coatings are based on the use of nickel-base superalloys and little data are available for coatings applied on cobalt-base superalloys. In view of this fact, this study/thesis was initiated to evaluate some aluminide coatings and their modifications on standard cobalt-base superalloys in low temperature hot corrosion and high temperature hot corrosion attack.

## II. EXPERIMENTAL PROCEDURE

### A. BACKGROUND

There are no significant differences in hot corrosion resistance between nickel-base superalloys and cobalt-base superalloys providing the effects of the specific alloying elements in the superalloys are considered. The formation of a sulfide phase in superalloys make the nickel-base alloys inferior to the cobalt-base system because of the formation of nickel sulfide phase which are active in destroying the corrosion resistance.

Cobalt-base superalloys do not have aluminum as a strengthening element and they are not alumina formers. Therefore, uncoated cobalt-base superalloys have to depend on a chromium oxide scale to achieve oxidation resistance. Obviously at the higher temperature the oxidation resistance of the cobalt-base superalloys are less than nickel-base superalloys which in general are alumina formers. In addition, when degradation begins, as the chromia scales become damaged, the less protective oxide formed on the nickel-base superalloys contain more nickel oxide as compared to cobalt oxide on cobalt-base superalloys. This conditions results in the more abrupt drop-off in oxidation resistance for cobalt-base superalloys than for nickel-base superalloys [Ref. 3: pp. 660-661].

For cobalt-base superalloys with less than about 20 percent chromium, the oxidation resistance is comparatively poor. Tungsten and molybdenum as refractory elements in cobalt-base superalloys have beneficial effects on the selective oxidation of chromium but when chromia is no longer formed the oxidation of these refractory metal elements results in increase oxidation due to the development of less protective oxide phases [Ref. 44].

From earlier investigations it is found that carbides in all superalloys are usually selectively attacked and the only protective scale is the formation of chromia over the carbides. However, often these scales are not protective because they crack. Therefore carbides in superalloys are sites of excessive oxidation. The carbides in superalloys should preferably be small and discontinuous for minimizing this type of degradation.

The laboratory furnaces in the Material Science Laboratories at the Naval Postgraduate School have been demonstrated to reproduce the morphology of cobalt-base superalloys degradation found in marine environments for both low temperature hot corrosion and high temperature hot corrosion. Pressurized burner rigs and simple burner rigs are two others widely used test methods. The most complex method which shows a good simulation of hot corrosion conditions is a pressurized burner rig which also induces low



temperature hot corrosion and high temperature hot corrosion conditions. However, the necessity of controlling the pressure, velocities, composition, and temperature of the hot corrosion airfoil environment results in increased testing time and cost. Simple burner rigs greatly reduce the cost of equipment and engine degradation modes are simulated using higher contaminant levels and increased testing times [Ref. 45].

For the NPS furnace test, prior to inserting the samples into the furnace, the samples are covered with a thin layer of contaminant salts and then an air/sulfur dioxide gas mixture flows through the furnace which is set at the temperature required. For low temperature hot corrosion and high temperature hot corrosion testing the temperatures are 700 and 900 C respectively, with a deviation of plus/minus 5 C. The weight of the salt layer applied is different for LTHC and HTHC testing. Using the pre-applied salt layer greatly reduces the time required for the initiation stage to occur. For low temperature hot corrosion testing the furnace is able to generate the hot corrosion attack in about 60 hours with results in the form of degradation morphology and relative ranking compare to either achieved by pressurized or simple burner rigs [Ref. 46]. Sufficient high temperature hot corrosion attack is produced in 200 hours of testing.

## B. HOT CORROSION TESTING

For this study four standard cobalt-base superalloys were selected. The various coatings evaluated on these alloys are listed in Table II. The compositions of these four standard cobalt-base superalloys along with a nickel-base superalloy (IN-738), as a control sample, are listed in Table III [Ref. 48]. The manufacturing processes of the various coatings on these four standard cobalt-base superalloys are listed in Table IV.

The coated specimens which are received in pins form of approximately 0.5 cm diameter are cut to a length of about 1.5 cm. The first step is to heat the pins at a temperature of 170 C for fifteen minutes in order to evaporate any moisture. The specimens are then reheated at the same temperature for about ten minutes in order to facilitate the application of an even salt layer on the surface. A salt solution with a concentration of 63.1 grams sodium sulfate and 39.1 grams magnesium sulfate in one liter of water is applied to the surface. Pins are then reheated in order to evaporate the water and are then reweighed. This step which is called salt treatment is repeated until the pin surface is covered with 1.5 milligrams of salt per square centimeter for low temperature hot corrosion testing and 2.0 milligrams of salt per square centimeter for high temperature hot corrosion testing.

The next step, after the first 'salting' is completed is to place the pins into the furnace set at 700 and 900 C for low temperature hot corrosion (LTHC) and high temperature hot corrosion (HTHC) testing, respectively. A mixture of air and sulfur dioxide with a flow rate of 2000 milliliters per minute and 5 milliliters per minute, respectively, is flowed over the pin's surface. After twenty hours the pins are taken out of the furnace examined visually and then resalted and returned to the furnace for additional testing. Three twenty hour cycles for a total of sixty hours testing is used for LTHC while ten twenty hour cycles for a total of two-hundreds hours testing is used for HTHC.

The tested and as-received control specimens were carefully cut, mounted and polished for optical and scanning electron microscope (SEM) analysis. Surface attack depth on each specimen was measured every 20 degrees around the circumference using the Aprigliano technique [Ref. 47]. The HTHC and LTHC data are listed in Table V and depicted graphically in Figure B.2. Where possible, three separate test section were examined for each coating test point. The data reported are the average of 36 (2 tests) and 54 (3 tests) measurements.

A scanning electron microscope (SEM) was used to examine the coating structure. The greater depth of field possible with the SEM was valuable in detailing the specific nature

of the attack on the different systems. Prior to using the SEM the specimens sections are coated with a thin gold layer and then silver liquid is used to connect the surface and the aluminum holder in order to have good electrical conductivity. These photomicrographs presented in Figure B.12-B.25, show the coating layer before and after hot corrosion testing .

### III. RESULTS AND DISCUSSION

#### A. HOT CORROSION RESISTANCE OF VARIOUS COATINGS ON MAR-M-509 SUBSTRATE.

The level of hot corrosion attack of the various coatings on the MAR-M-509 substrate can be seen in Figure B.3. The Std-Al coating has a higher attack (15 microns) at high temperature than at low temperature (13 microns). The difference between these two attacks is in a small range. Figure B.12 shows typical SEM photomicrographs of the as-received, LTHC, and HTHC test specimens with the Std-Al coating on MAR-M-509 substrate. It can be seen that the standard aluminide coating has a three zone structure similar to that observed on nickel-base superalloys [Ref. 5]. Unfortunately, the phase identification of this coating on cobalt-base superalloys has not yet been investigated. There is no significant hot corrosion attack on this coating at both high and low temperatures.

The Pt-Al coating has a higher amount of attack at high temperature than at low temperature (18 microns). At the high temperature, the coating failed after only 60 hours of testing. At both high and low temperatures, the Pt-Al coating showed higher attack than the Std-Al coating. Figure B.13 shows typical SEM photomicrographs of the Pt-Al coating in which the three zone structure is shown. It can



be seen that there is attack at high temperature where a small part of the surface zone has been depleted. At low temperature, the attack occurs under the surface zone which shows pitting, a characteristic of the LTHC attack.

The Pt-Cr-Al coating has a higher attack (22 microns) at high temperature than at low temperature (20 microns). The difference between these two penetrations is as described with the Std-Al coating. At both high and low temperatures, the Pt-Cr-Al coating showed higher attack than either the Std-Al or the Pt-Al coatings. Figure B.14 shows typical SEM photomicrographs of the Pt-Cr-Al coating with its three zone structure. There is no significant hot corrosion attack evident in this section.

The CVD-Low Al coating has a lower amount of attack (12 microns) at high temperature than at low temperature (16 microns) although the difference between these two attacks is small. This coating has a lower attack than the Std-Al, Pt-Al, or Pt-Cr-Al coatings at high temperature. At low temperatures, the attack is less than for the Pt-Al and Pt-Cr-Al coatings. Figure B.15 shows typical SEM photomicrographs of the CVD-Low Al coating. It can be seen that there is a less defined three zone structure. There is no significant attack can be observed at high temperatures.

The Rh-Al coating has a higher hot corrosion attack (41 microns) as compared to the attack of other coatings on the

MAR-M-509 substrate at high temperature. The Rh-Pt-Al coating has the same hot corrosion attack (12 microns) as the unmodified CVD-Low Al coating both tested at high temperature. Figure B.16 shows typical SEM photomicrographs of the Rh-Al and Rh-Pt-Al coatings at high temperature, respectively. Because of a lack of specimens no low temperature testing were performed.

#### B. HOT CORROSION RESISTANCE OF VARIOUS COATINGS ON X-40 SUBSTRATE.

Hot corrosion attack results of the various coatings on the X-40 substrate can be seen in Figure B.4. The Std-Al coating has a higher hot corrosion attack (27 microns) at high temperature than at low temperature (12 microns). The difference between these two attacks is fairly large (15 microns) but it is still lower than the difference observed on nickel-base superalloys (IN-738 as a control sample). Figure B.17 shows typical SEM photomicrographs of the Std-Al coating where the three zone structure is clearly shown. No significant attack can be observed in this particular section. As mentioned earlier, no work has been done with X-Ray diffraction analysis to identify the phases present in the various coatings on cobalt-base superalloys.

The Pt-Al coating has a lower hot corrosion attack (13 microns) at high temperature than at low temperature (16 microns) although the difference between these is quite

small. This coating has a lower attack than the Std-Al coating at high temperature. At low temperature the attack is higher than that observed for the Std-Al coating. Figure B.18 shows typical SEM photomicrographs of the Pt-Al coating where the three zone structure is clearly shown and there is no significant attack can be observed.

The Pt-Cr-Al coating has the same hot corrosion attack (28 microns) at both high and low temperatures. This coating exhibited higher penetration than either the Std-Al or Pt-Al coatings in both high and low temperature testing. Figure B.19 shows typical SEM photomicrographs of the Pt-Cr-Al coating in which the three zone structure is shown. In the section presented it can be seen that the attack is significant at low temperature while no attack can be observed at high temperature.

#### C. HOT CORROSION RESISTANCE OF VARIOUS COATINGS ON FSX-414 SUBSTRATE.

Hot corrosion resistance of the various coatings on the FSX-414 substrate are presented in Figure B.5. The Std-Al coating has a higher attack (25 microns) at high temperature than at low temperature (21 microns). The difference between these two attacks is small. Figure B.20 shows typical SEM photomicrographs of the Std-Al coating where the attack can be seen on the low temperature exposed specimen.

The Pt-Al coating has a lower attack (11 microns) at high temperature than at low temperature (20 microns). The difference between these two attacks is relatively small. The Pt-Al coating has a lower attack than the Std-Al coating at high temperature but it showed a comparable level of attack at the low temperature. Figure B.21 shows typical SEM photomicrographs of the Pt-Al coating in which the three zone structure is clearly shown. Also, the characteristic of the LTHC attack can be seen clearly here. No significant attack can be observed at high temperature.

The Pt-Cr-Al coating has a lower attack (8 microns) at high temperature than at low temperature (15 microns). The Pt-Cr-Al coating has lower attack than the Std-Al and Pt-Al coatings at both high and low temperatures. Figure B.22 shows typical SEM photomicrographs of the Pt-Cr-Al coating in which the three zone structure is clearly shown. At low temperature, the surface zone above the attack area has been depleted.

At high temperature, the Rh-Pt-Al coating has a higher attack (16 micron) than the Pt-Cr-Al and Pt-Al coatings but it is lower than that observed on the Std-Al coating. Figure B.23 shows typical SEM photomicrographs of the Rh-Pt-Al coating at high temperature. The three zone structure is clearly shown and there is a small attack in the surface zone.

D. HOT CORROSION RESISTANCE OF VARIOUS COATINGS ON WI-52 SUBSTRATE.

Hot corrosion attack data of the various coatings on the WI-52 substrate can be seen in Figure B.6. At high temperature, the aluminide pack process coating has equivalent attack (19 microns) than the attack (18 micron) on the Rh-Al coating. As stated earlier, there were no specimens available for LTHC testing. Figure B.24 shows typical SEM photomicrographs of these two coatings at high temperature. The three zone structure is not shown in this figure. Instead the so called rumpling, a form of surface plastic instability, seems to appear. This is also observed for the Pt-Al coating on the IN-738 substrate [Ref. 33].

E. HOT CORROSION RESISTANCE OF EB-PVD COBALT CHROMIUM ALUMINUM YTTRIUM AND PLATINUM-ALUMINIDE COATINGS ON IN-738 AS CONTROL SAMPLE.

Hot corrosion attack results of the Rh-Pt-Al and Pt-Al coatings on the IN-738 substrate can be seen in Figure B.6. There is no hot corrosion attack observed on the Rh-Pt-Al coating, while for the Pt-Al coating, the attack is 65 microns at high temperature. At low temperature, the Rh-Pt-Al overlay coating also showed no hot corrosion attack although for some compositions (particularly for the lower Cr levels) LTHC attack is found [Ref. 49]. The Pt-Al coating has a higher attack (65 microns) at high temperature than at low temperature (14 microns). The difference



between these two attacks (51 micron) is quite large when compared to the coating differences observed on the other cobalt-base superalloys. The Pt-Al coating on the IN-738 substrate has much higher attack than on cobalt-base superalloys at the high temperature. There is less attack evident at low temperature for the Pt-Al coating on IN-738 than there is for the same coating on the MAR-M-509, X-40 and FSX-414 substrates which is also quite surprising. Figure B.25 shows typical SEM photomicrographs of the Rh-Pt-Al and Pt-Al coatings on the IN-738 substrate. It can be seen that the Rh-Pt-Al coating is still in good condition which is also shown in Table V. At high temperature the attack on the Pt-Al coating has penetrated into the substrate. No significant attack can be observed at LTHC.

#### F. STANDARD ALUMINIDE COATING ON VARIOUS SUPERALLOYS.

The hot corrosion resistance of the Std-Al coating on the various cobalt-base substrates can be seen in Figure B.7. On the MAR-M-509 substrate this coating has only a slightly higher attack (15 microns) at high temperature than at low temperature (13 microns).

The Std-Al coating on the X-40 substrate has a higher attack (27 microns) at high temperature than at low temperature (12 microns). The difference between these two levels of penetration (15 microns) is larger than that observed on the MAR-M-509 substrate. On the X-40 substrate, the Std-Al

coating has a higher attack than on the MAR-M-509 substrate at high temperature. At low temperature the attack is equivalent to that observed on the MAR-M-509 substrate.

The Std-Al coating on the FSX-414 substrate has a higher attack (25 microns) at high temperature than at low temperature (21 microns). The difference between these two attacks (4 microns) is slightly larger compared to the difference on the MAR-M-509 substrate but smaller than that on the X-40 substrate. The Std-Al coating on the FSX-414 substrate has higher attack than on the MAR-M-509 substrate and lower attack than on X-40 substrate at high temperature. At low temperature the attack is higher than that observed on both the MAR-M-509 and X-40 substrates.

#### G. PLATINUM ALUMINIDE COATING ON VARIOUS SUPERALLOYS.

The hot corrosion resistance results of the Pt-Al coating on the various cobalt-base substrates can be seen in Figure B.8. The Pt-Al coating on the MAR-M-509 substrate failed after only 60 hours of testing while the attack is 18 microns at low temperature.

The Pt-Al coating on the X-40 substrate has a slightly lower attack (13 microns) at high temperature than at low temperature (16 microns). The difference between these two penetrations is small. At high temperature, this coating experiences lower attack on the X-40 substrate than on the MAR-M-509 substrate. At low temperature the attack is lower than the attack observed on the MAR-M-509 substrate.

The Pt-Al coating on the FSX-414 substrate has a lower attack (11 microns) at high temperature than at low temperature (20 microns). The difference between these two attacks (9 microns) is larger than the difference observed on the X-40 substrate. At high temperature the Pt-Al coating on the FSX-414 substrate sustained a lower attack than it did on the X-40 and MAR-M-509 substrates. At low temperature the attack is higher than that observed on the MAR-M-509 and X-40 substrates.

#### H. PLATINUM CHROMIUM ALUMINIDE COATING ON VARIOUS SUPERALLOYS.

The level of hot corrosion resistance of the Pt-Cr-Al coating on the various cobalt-base substrates can be seen in Figure B.9. The Pt-Cr-Al coating on the MAR-M-509 substrate exhibits only slightly higher attack (22 microns) at high temperature than at low temperature (20 microns).

The Pt-Cr-Al coating on the X-40 substrate has the same attack (28 microns) at both high and low temperatures. The Pt-Cr-Al coating on the X-40 substrate has higher attack than it does on the MAR-M-509 substrate at high temperature. At low temperature the attack is higher than for the same coating on the MAR-M-509 substrate.

The Pt-Cr-Al coating on the FSX-414 substrate has lower attack (8 microns) at high temperature than at low temperature (15 microns). The difference between these two attacks

(7 microns) is large as compared to the difference on the MAR-M-509 and X-40 substrates. At both high and low temperature, this coating has lower attack than the same coating on the MAR-M-509 and X-40 substrates.

#### I. RHODIUM-ALUMINIDE COATING ON MAR-M-509 AND WI-52 SUBSTRATES.

The hot corrosion resistance of the Rh-Al coating on the MAR-M-509 and FSX-414 substrates can be seen in Figure B.10. The Rh-Al coating has higher attack on the MAR-M-509 substrate than on the WI-52 substrate at high temperature. No specimens were available for low temperature testing.

#### J. RHODIUM-PLATINUM-ALUMINIDE COATING ON MAR-M-509 AND FSX-414 SUBSTRATES.

The hot corrosion resistance of the Rh-Pt-Al coating on the MAR-M-509 and FSX-414 substrates can be seen in Figure B.11. At high temperature the Rh-Pt-Al coating has lower attack on the MAR-M-509 substrate than on the FSX-414 substrate. No specimens were available for low temperature testing.

In this study, the initial differences between the aluminide pack process and CVD-Low Al coatings on the various cobalt-base substrates were neither tested nor compared.

In general, the addition of modifying elements such as Cr and/or Pt, Rh, to aluminide provided little benefit.

This may be the result of the cobalt and high chromium level of the substrate which in general are believed to provide superior hot corrosion resistance to the lower Cr and nickel-base alloys. In other studies the sequencing and coating processing steps was found to be very important. This aspect has not been explored in this study and deserves additional attention.

For the unmodified aluminide coatings, processing and the resulting structural difference had a significant effect on protectivity. The low aluminum activity CVD applied coating appears to have the best protectivity. Because of the difficulty of aluminizing the aluminum free cobalt-base superalloys, the apparent benefit of the low aluminum activity process may be in the structural stability of the resulting coating. The inner coating zone is less discrete and offer greater resistance to spalling.

For many coating systems, particularly the diffusion aluminide, the substrate has a strong influence on protectivity. In general, in this study of cobalt-base superalloys only small effects or differences were found even though a wide range of compositions were studied. As previously noted, possibly the universally high chromium levels, greater than 20 percent and the cobalt effect or nickel are overriding factors. This effect may help explain why only minimum benefits of additional elements were seen for the



cobalt coating systems while large effects are found on the nickel-base alloys.

In hot corrosion testing of nickel-base coating systems under low and high temperature conditions, large differences in attack morphology, degradation mechanisms, and rate of penetration are generally observed. For the coating systems studied on cobalt-base alloys in this program, much smaller differences in rate of attack were measured although similar degradation modes were observed to be operating. LTHC was still the more aggressive environment. Here chromium level is most beneficial and the high chromium level of the substrates may overshadow any additional benefits of the coating modification evaluated.

#### IV. CONCLUSIONS AND RECOMMENDATIONS

Based on the initial study of the various aluminide coating types on four cobalt-base superalloys, the following conclusions can be drawn :

1. On the MAR-M-509 substrate, the CVD-Low Al and Rh-Pt-Al coatings are more effective for high temperature hot corrosion (HTHC) resistance while the Std-Al coating is more effective for low temperature hot corrosion (LTHC) resistance.
2. On the X-40 substrate, the CoCrAlY overlay coating is more effective for high temperature hot corrosion resistance while the Std-Al coating is more effective for low temperature hot corrosion resistance.
3. On the FSX-414 substrate, the Pt-Cr-Al coating is the most effective for both high and low temperatures hot corrosion resistance.
4. On the WI-52 substrate, the aluminide pack process and Rh-Al coatings are comparable for high temperature hot corrosion resistance.
5. The Std-Al coating is more effective on the MAR-M-509 substrate than it is on the X-40 and FSX-414 substrates for high temperature hot corrosion resistance. At low temperature, this coating is more effective on both MAR-M-509 and X-40 than on FSX-414 substrates.
6. The Pt-Al coating is more effective on the FSX-414 substrate than on the MAR-M-509 and X-40 substrates for HTHC resistance. For LTHC resistance, this coating is more effective on X-40 than on both MAR-M-509 and FSX-414 substrates.
7. The Pt-Cr-Al coating is more effective on the FSX-414 substrate than on the MAR-M-509 and X-40 substrates for both HTHC and LTHC resistance.
8. The Rh-Al coating is more effective on WI-52 than on MAR-M-509 substrate for high temperature hot corrosion resistance.

9. The Rh-Pt-Al coating is more effective on MAR-M-509 than on FSX-414 substrates for high temperature hot corrosion resistance.
10. The HTHC and LTHC attack for the various coatings on cobalt-base superalloys varies overalls in a small range while the difference on nickel-base superalloys is in a large range.

This study is an initial attempt to investigate the effects of the various coatings on cobalt-base superalloys an area where few data are available. The following are some recommendations for future study :

1. The X-Ray Diffraction analysis of the various coatings on the four cobalt-base substrates studied in order to determine the phases present and better understand the structural features which so strongly affect protectivity of the substrate.
2. A comprehensive study of the coating structural properties should be conducted on the four cobalt-base substrates using the most effective coating systems identified in this thesis.
3. Further testing and more detailed analysis of the specific coating substrate combinations identified in this program.

# APPENDIX A : TABLES I-V

## TABLE I

### SUMMARY OF HOT CORROSION MECHANISMS

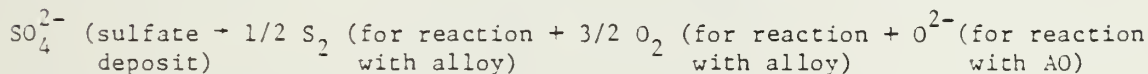
Possible Propagation Modes for Hot Corrosion of  
Superalloys by  $\text{Na}_2\text{SO}_4$  Deposits

I. Modes Involving Fluxing Reactions	II. Modes Involving A Component of the Deposit
<ul style="list-style-type: none"> <li>•Basic</li> <li>•Acidic</li> </ul>	<ul style="list-style-type: none"> <li>•Sulfur</li> <li>•Chlorine</li> </ul>

#### I. Fluxing Modes

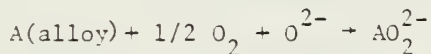
##### A. Basic Processes

1. Dissolution of Reaction Product Barriers, (i.e. AO) Due to Removal of Sulfur and Oxygen from the  $\text{Na}_2\text{SO}_4$  by the Metal or Alloy:



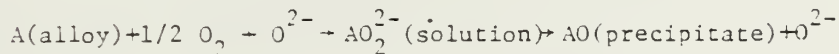
Reaction between AO and oxide ions can follow 2 courses:

- (a) Continuous dissolution of AO



$\text{Na}_2\text{SO}_4$  is converted to  $\text{Na}_2\text{AO}_2$  and attack is dependent on amount of  $\text{Na}_2\text{SO}_4$  initially present.

- (b) Solution and reprecipitation



A supply of  $\text{SO}_3$  is required in order for attack to proceed indefinitely, otherwise attack will stop when melt becomes sufficiently basic at precipitation site.

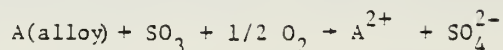
Table I

## Summary of hot corrosion mechanisms (cont'd)

B. Acidic Processes

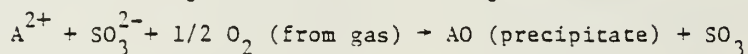
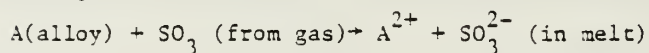
## 1. Gas Phase Induced

- (a) Formation of
- $ASO_4$
- in
- $Na_2SO_4$
- :



Continuous solution of  $ASO_4$  in  $Na_2SO_4$  requires continuous supply of  $SO_3$  and  $O_2$  from gas.

- (b) Solution and Precipitation of AO in
- $Na_2SO_4$
- Due to Reduction of
- $SO_3$
- :



- (c) Nonprotective Reaction Product Barrier formation due to rapid removal of base element (e.g. Co, Ni) from alloy by molten deposit (33).

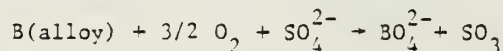
- (d) Solution and Precipitation of AO as a Result of Negative Gradient in Solubility of AO in
- $Na_2SO_4$
- as in B.

## 2. Alloy Phase Induced

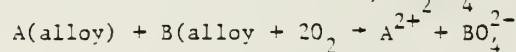
- (a) Solution of AO in
- $Na_2SO_4$
- Modified by Second Oxide from Alloy (i.e.
- $BO_3$
- ).

Sequence:

- i. Modification of
- $Na_2SO_4$
- by
- $BO_3$

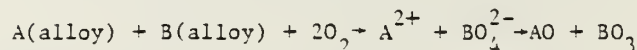


- ii. Solution reaction for AO,
- $Na_2SO_4$
- becomes enriched in
- $ABO_4$

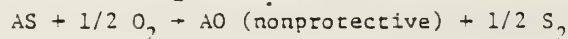
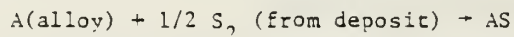


or

- iii. Solution and reprecipitation

II. Salt Component Effects

## A. Sulfur



## B. Chlorine





TABLE 2  
LIST OF SPECIMENS

SPECIMEN NUMBER	SUBSTRATE USED	COATING APPLIED
1	MAR-M-509	Std-Al
2	MAR-M-509	Pt-Al
3	MAR-M-509	Pt-Cr-Al
4	MAR-M-509	CVD-Low Al
5	MAR-M-509	Rh-Al
6	MAR-M-509	Rh-Pt-Al
7	X-40	Std-Al
8	X-40	Pt-Al
9	X-40	Pt-Cr-Al
10	X-40	EB-PVD CoCrAlY
11	FSX-414	Std-Al
12	FSX-414	Pt-Al
13	FSX-414	Pt-Cr-Al
14	FSX-414	Rh-Pt-Al
15	WI-52	aluminide pack process
16	WI-52	Rh-Al
17	IN-738	EB-PVD CoCrAlY
18	IN-738	Pt-Al

TABLE 3

## NOMINAL COMPOSITION (WT.%) OF CAST SUPERALLOYS

ELEMENT	SUBSTRATE				
	MAR-M-509	X-40	FSX-414	WI-52	IN-738
C	.60	.50	.25	.45	.17
Mn	.10(c)	.50	1.00(c)	.50	.20
Si	.10(c)	.50	1.00(c)	.50(c)	.30
Cr	21.50	25.00	29.50	21.00	1.60
Ni	10.00	10.00	10.50	1.00(c)	Bal
Co	Bal	Bal	Bal	Bal	8.50
Mo	-	-	-	-	1.75
W	7.00	7.50	7.00	11.00	2.60
Cb	-	-	-	2.00	0.90
Ti	.20	-	-	-	3.40
Al	-	-	-	-	3.40
B	.01(c)	-	.012	-	.01
Zr	.50	-	-	-	.10
Fe	1.00	1.50	2.00(c)	2.00	.50
Other	3.50 Ta	-	-	-	1.75

(c) - Maximum Composition

TABLE 4  
COATING MANUFACTURING PROCESS

Coating	Process
Std-Al	1) Diffuse at 1080 C for 8 hours 2) Aluminizing - HTLA Process
Pt-Al	1) Platinizing (5-10 um) - Electroplating 2) Diffuse at 870 C for 4 hours 3) Aluminizing - HTLA Process 4) Diffuse at 1080 C for 8 hours
Pt-Cr-Al	1) Platinizing (5-10 um) - Electroplating 2) Chromizing - Pack Cementation at 1060 C for 7 hours 3) Aluminizing - HTLA Process 4) Diffuse at 1080 C for 8 hours
Aluminide	1) Aluminizing -Pack Process 2) Diffuse at 1040 C for 4 hours
CVD-Low Al	Aluminizing - CVD Process ( not in the Pack ) - Low Activity lead
EB-PVD CoCrAlY	1) Overlay Coating Applied by EB-PVD technique 2) Medium Cr (22 %)
Rh-Al	1) Rh Modified Aluminide 2) Aluminizing - Pack Cementation Process
Rh-Pt-Al	1) Rh and Pt Modified Aluminide 2) Aluminizing - Pack Cementation Process

CVD = Chemical Vapor Deposition

EB-PVD = Electron-Beam Physical Vapor Deposition

TABLE 5

## RESULTS OF HOT CORROSION DATA

Specimen number	High Temp. (900 C) Depth of Attack, um			Low Temp. (700 C) Depth of Attack, um		
	Min.	Max.	Ave.	Min.	Max.	Ave.
1	10	60	15 ± 17	0	30	13 ± 6
2	-	-	failed	0	80	18 ± 9
3	30	60	22 ± 6	0	60	20 ± 11
4	20	50	12 ± 6	0	20	16 ± 5
5	60	100	41 ± 7	-	-	-
6	20	30	12 ± 2	-	-	-
7	50	60	27 ± 2	0	20	12 ± 6
8	0	40	13 ± 9	0	60	16 ± 8
9	30	110	28 ± 12	0	50	28 ± 13
10	0	15	2 ± 0	0	20	14 ± 5
11	30	70	25 ± 6	0	30	21 ± 8
12	0	40	11 ± 7	0	30	20 ± 7
13	0	20	8 ± 3	0	30	15 ± 8
14	20	60	16 ± 7	-	-	-
15	30	70	19 ± 7	-	-	-
16	10	70	18 ± 9	-	-	-
17	0	0	0 ± 0	-	-	-
18	90	180	65 ± 22	0	20	14 ± 5

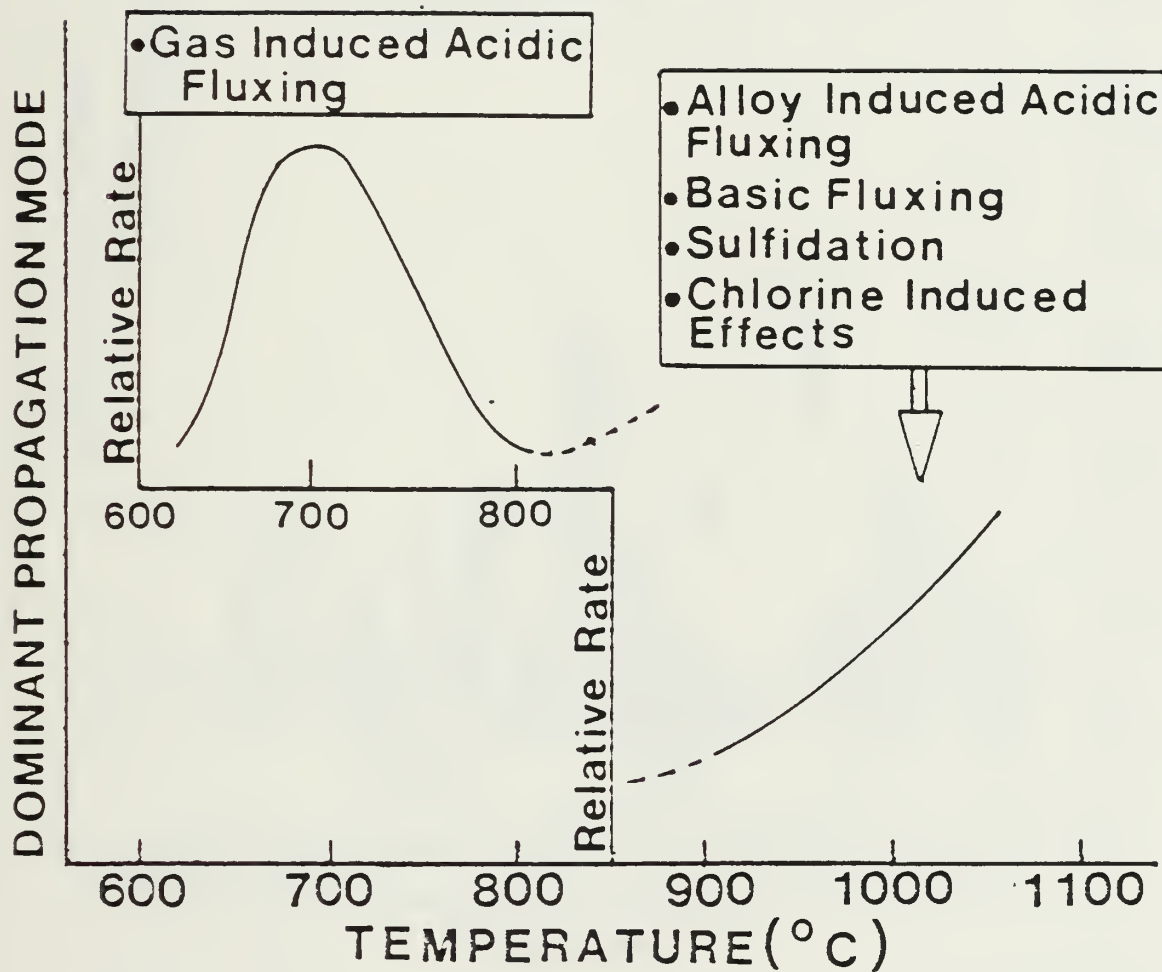


Figure B.1 Relative rates of attack.



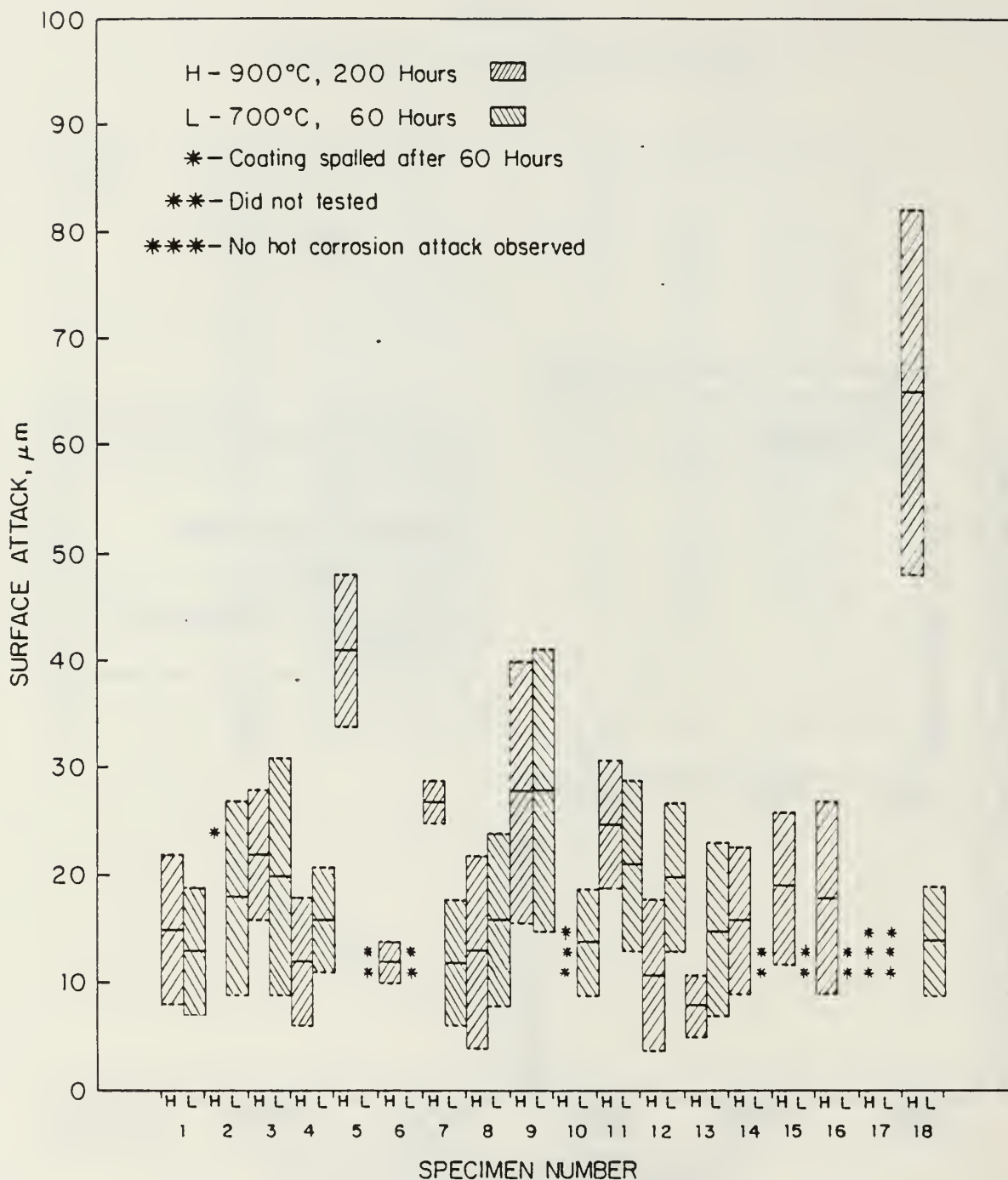


Figure B.2 Graphical representation of hot corrosion data at 900 and 700 C.

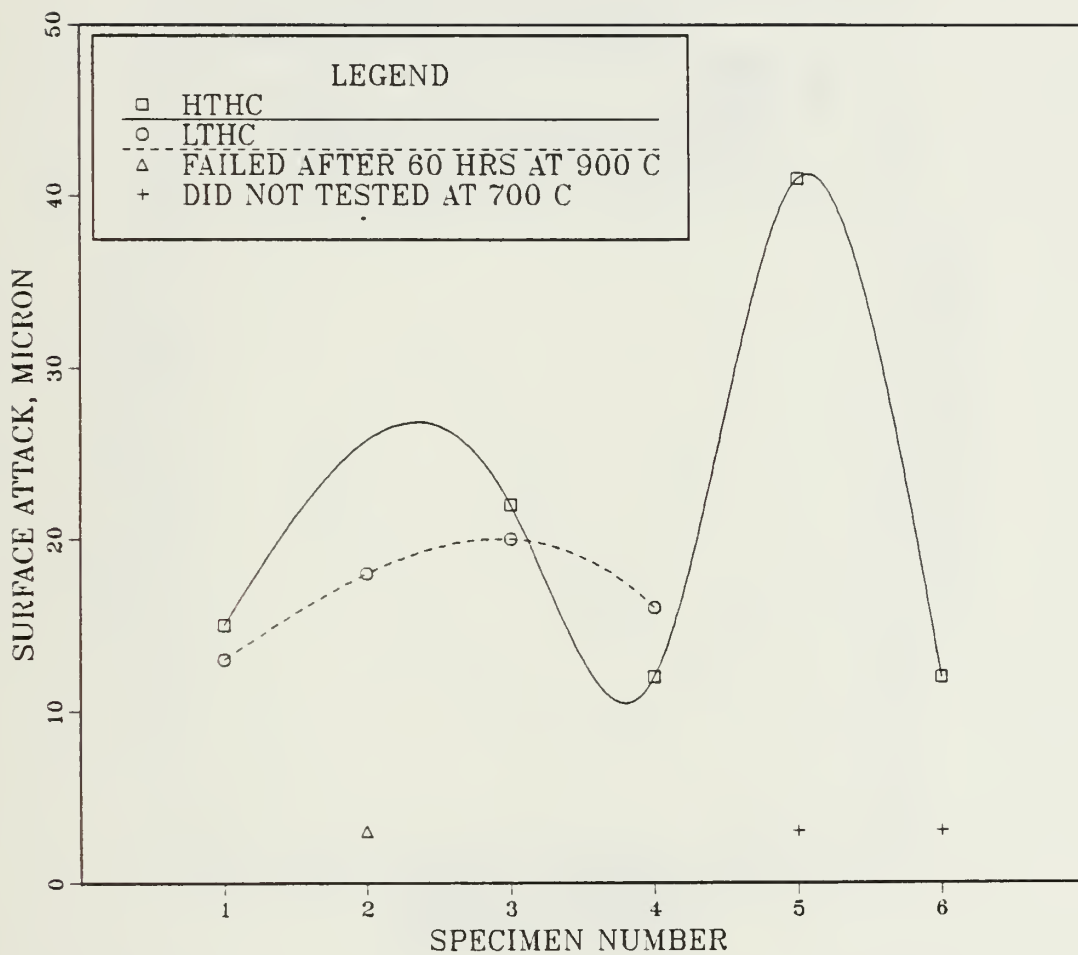


Figure B.1 High and low temperature hot corrosion behavior of various coatings on MAR-M-500 substrate.

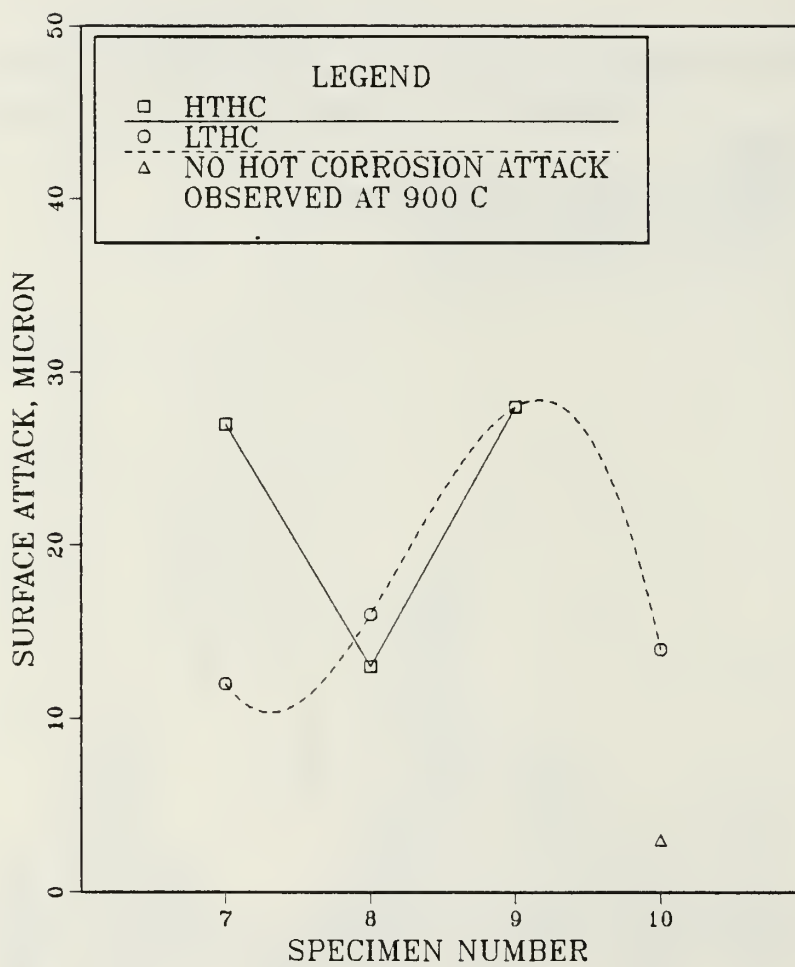


Figure B.4 High and low temperature hot corrosion behavior of various coatings on Z-40 substrate.

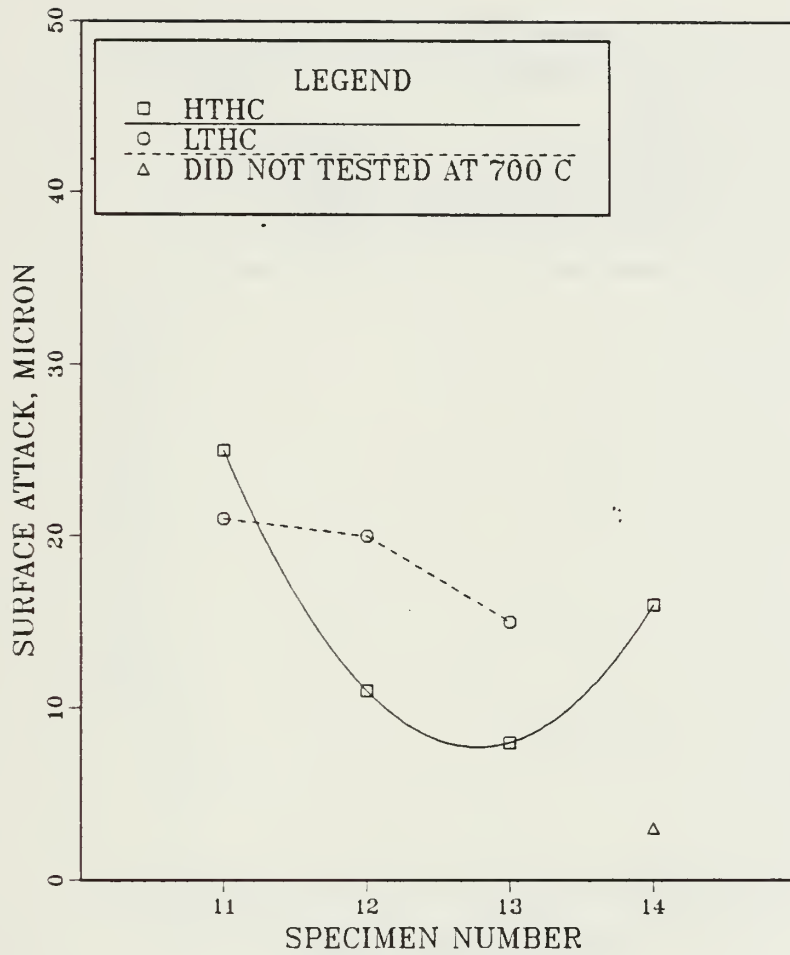


Figure B.5 High and low temperature hot corrosion behavior of various coatings on FSX-414 substrate.

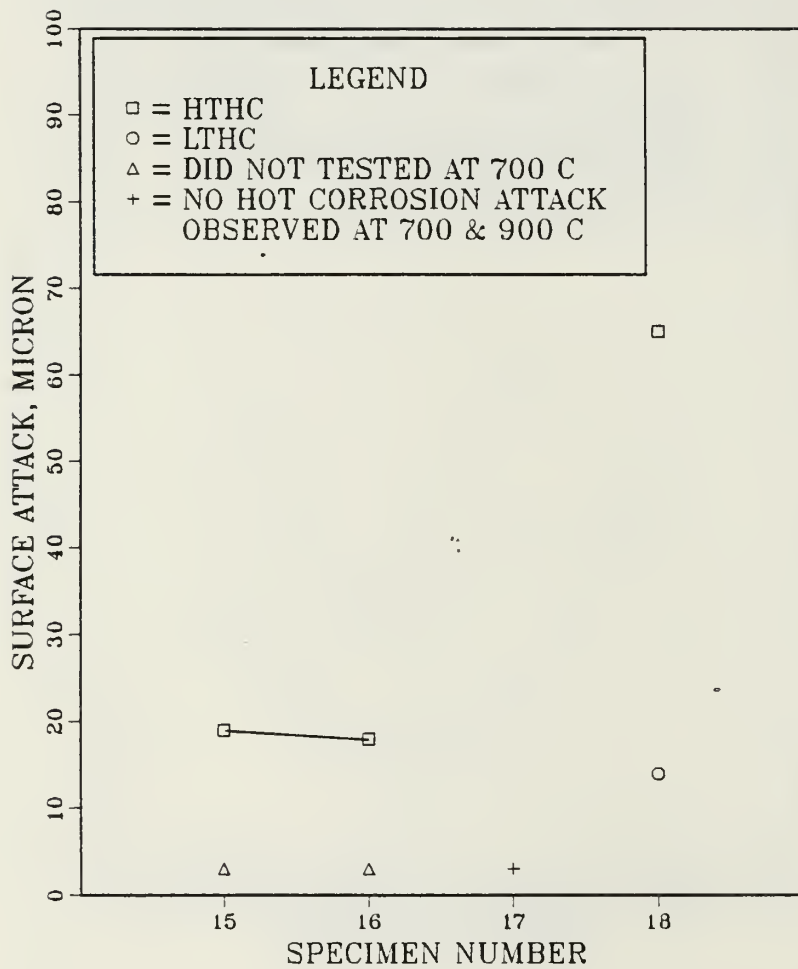


Figure B.6 High and low temperature hot corrosion behavior of various coatings on NI-52 and IN-738 substrates.



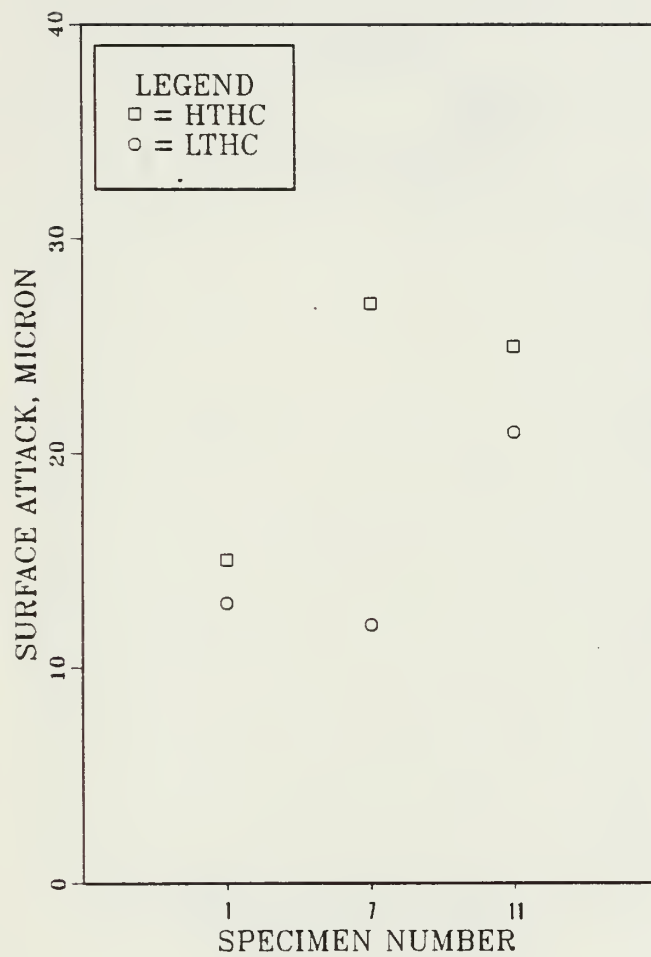


Figure B.7 Effects of Std-Al coatings on various superalloys.

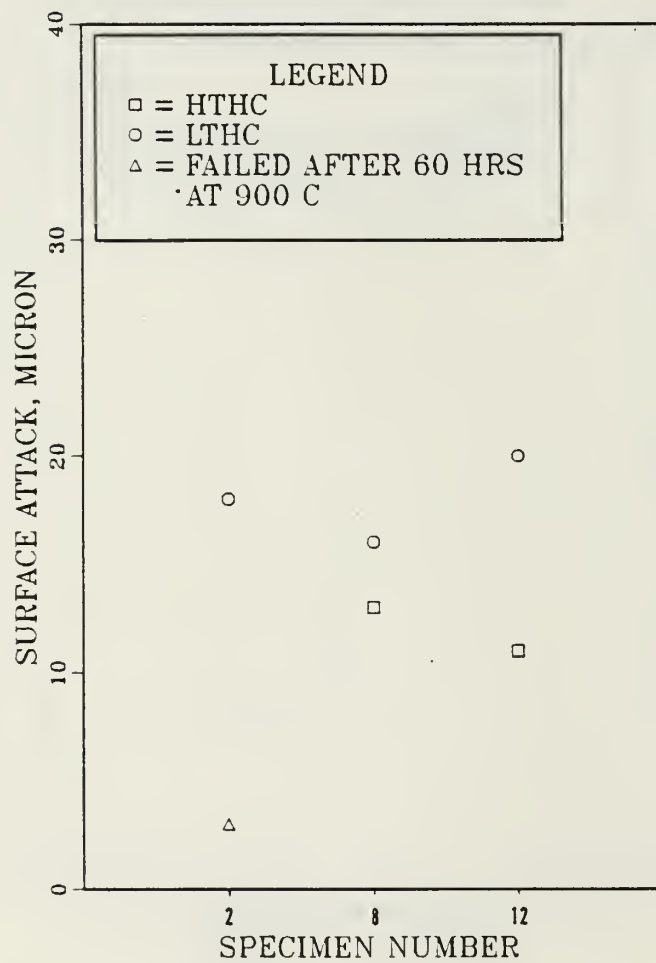


Figure B.8 Effects of Pt-Al coatings on various superalloys.

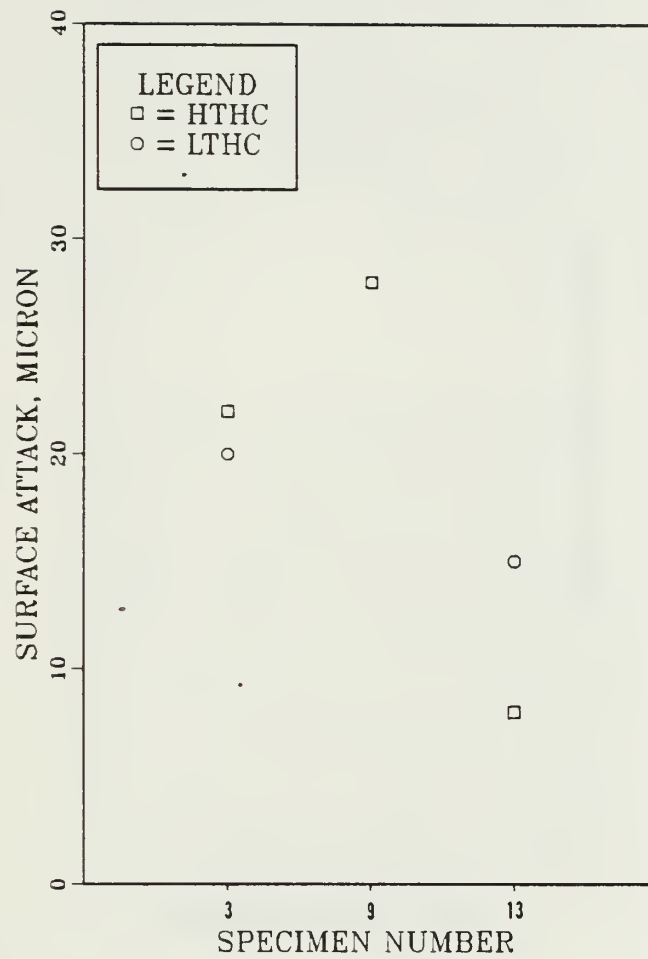


Figure B.9 Effects of Pt-Cr-Al coatings on various superalloys.

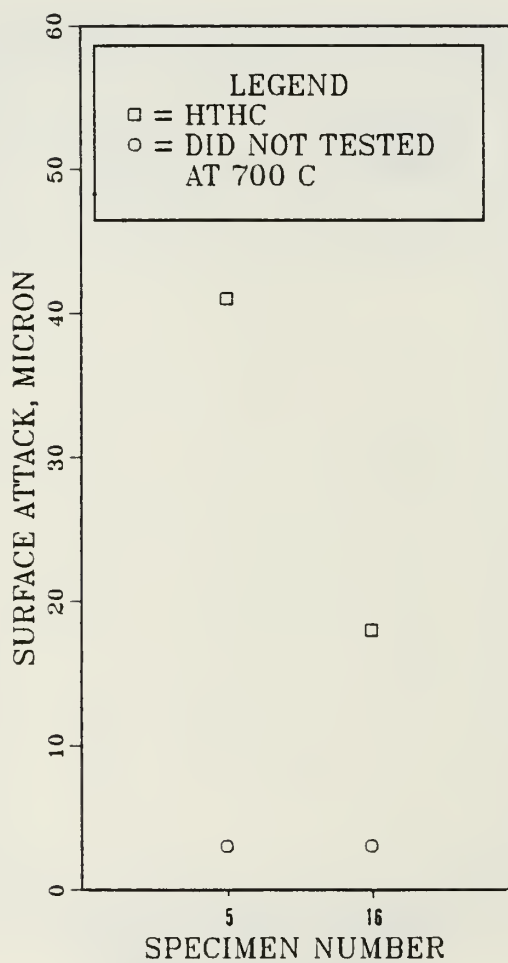


Figure B.10 Effects of Rh-Al coatings on MAR-M-509 and W-52 substrates.

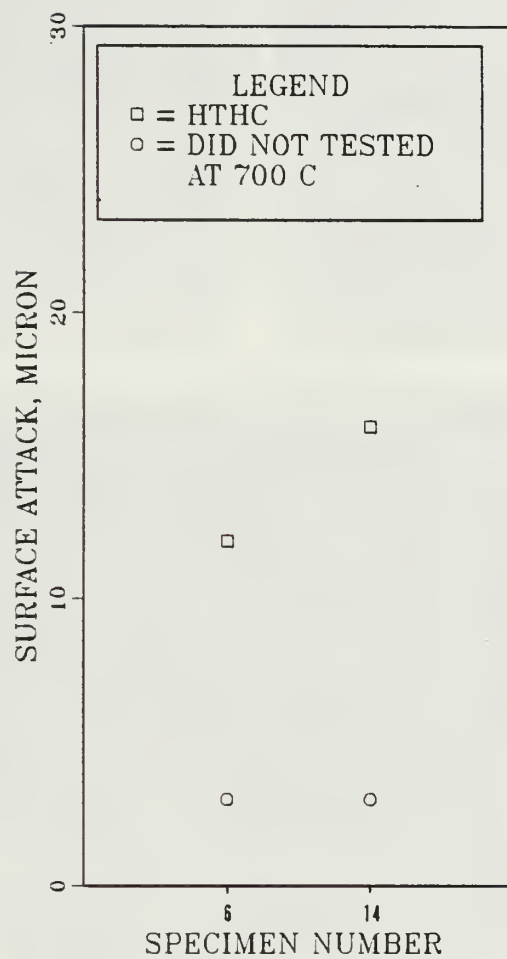


Figure B.11 Effects of Rh-Pt-Al coatings on NAR-14-509 and FSX-414 substrates.



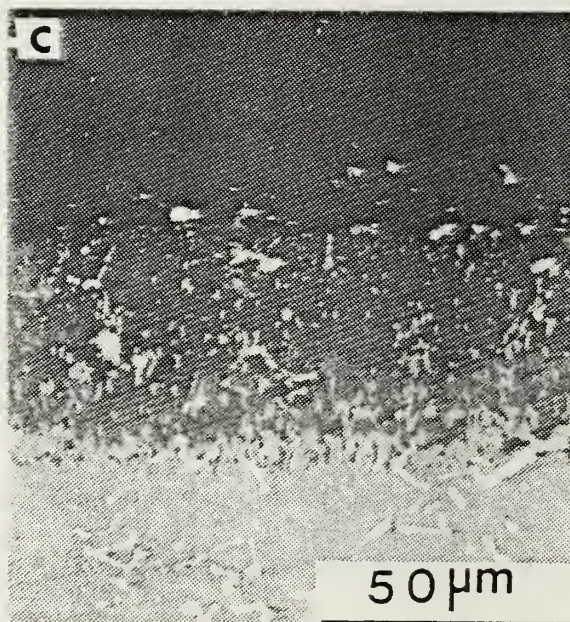
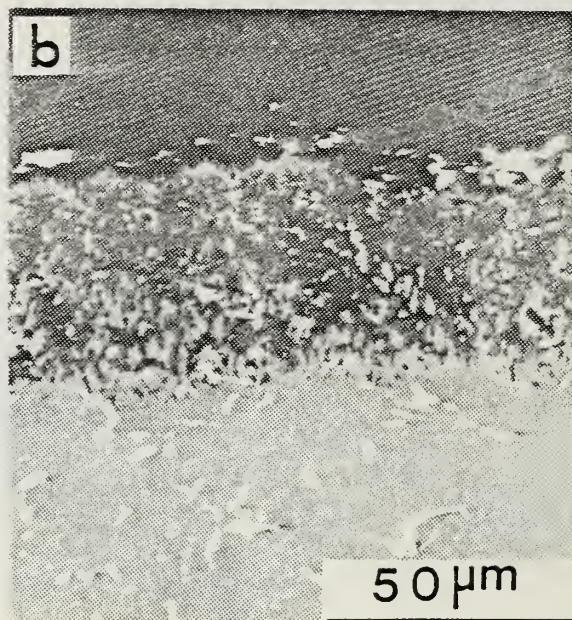
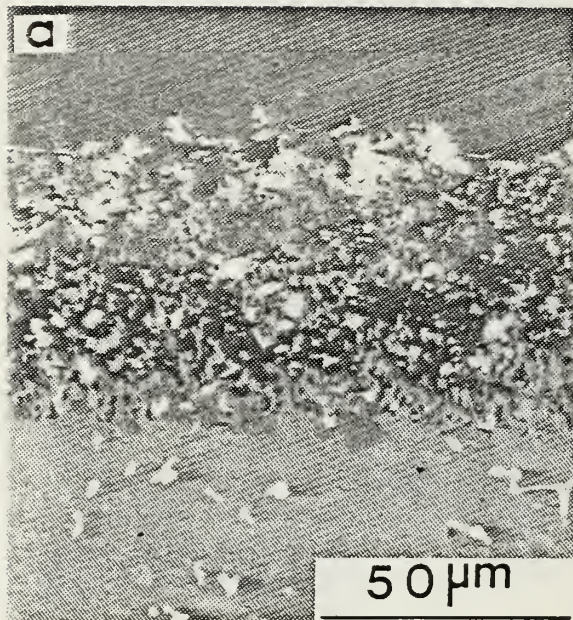


Figure B.12 SEM photomicrographs of Std-Al coatings on MAR-M-509 substrate: (a) exposed 200 hrs at 900 C, (b) exposed 60 hrs at 700 C and (c) as-received.



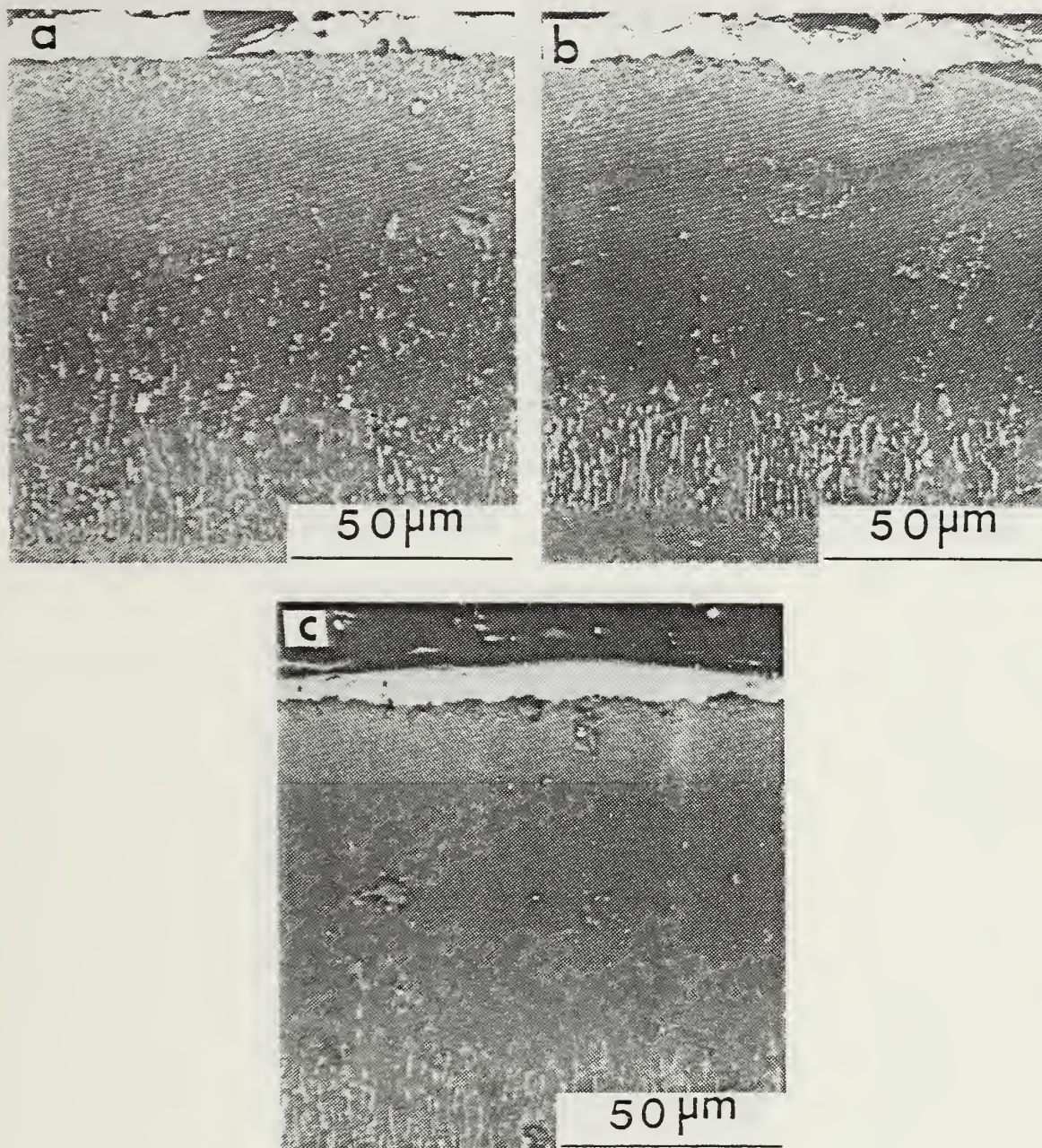


Figure B.13 SEM photomicrographs of Pt-Al coatings on MAR-M-509 substrate: (a) exposed 200 hrs at 900 C, (b) exposed 60 hrs at 700 C and (c) as-received.



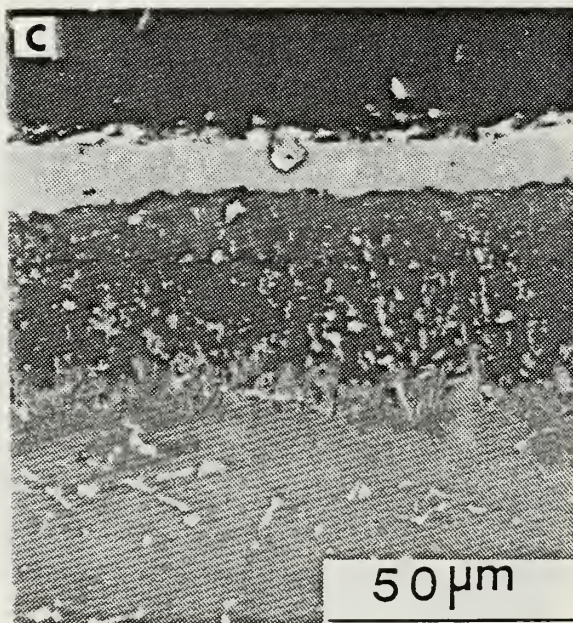
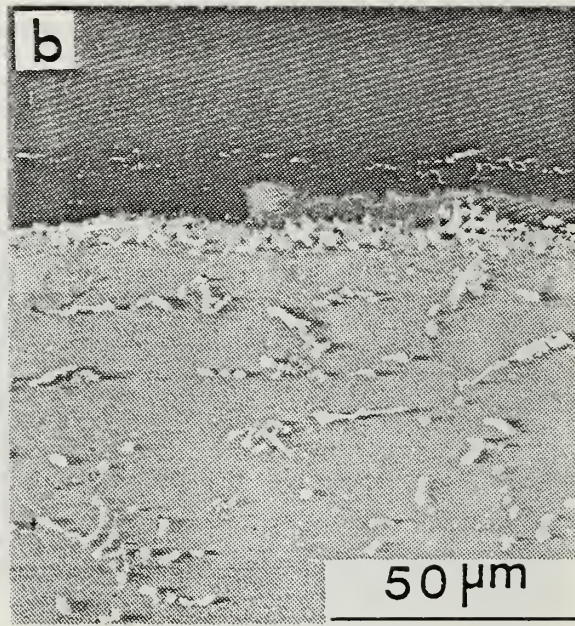
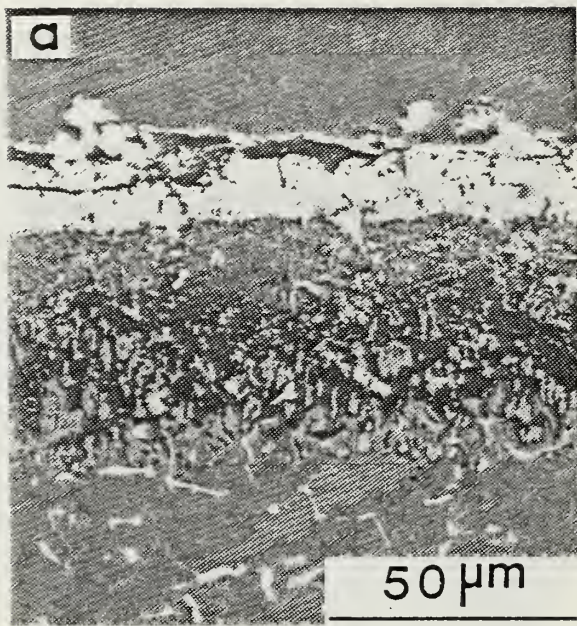


Figure B.14 SEM photomicrographs of Pt-Cr-Al coatings on MAR-M-509 substrate: (a) exposed 200 hrs at 900 C, (b) exposed 60 hrs at 700 C and (c) as-received.



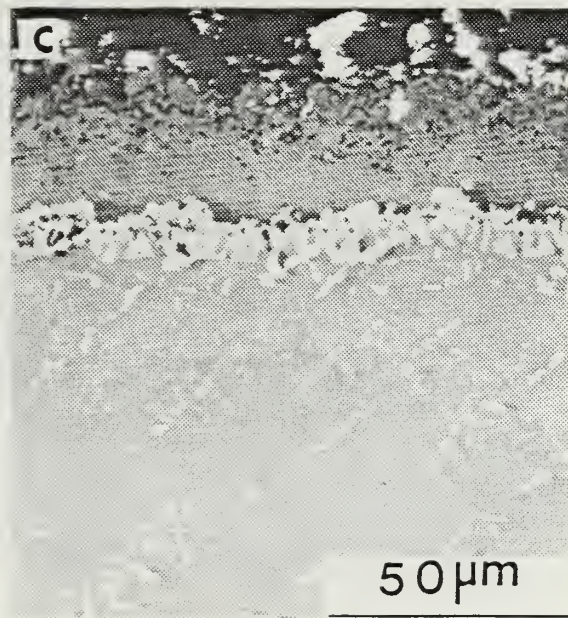
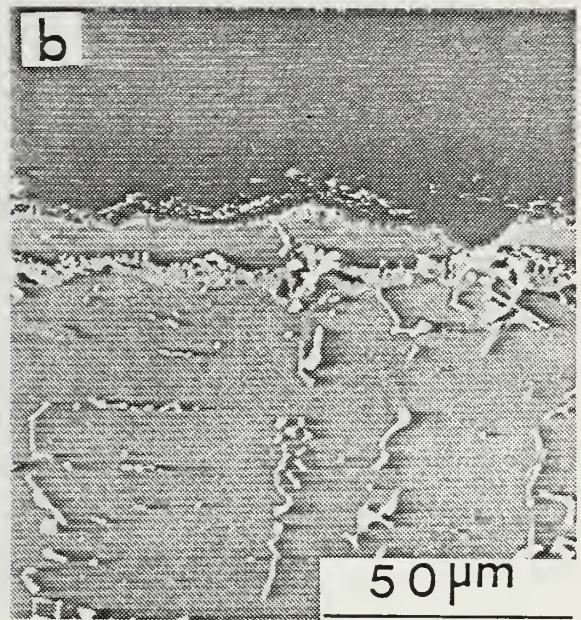
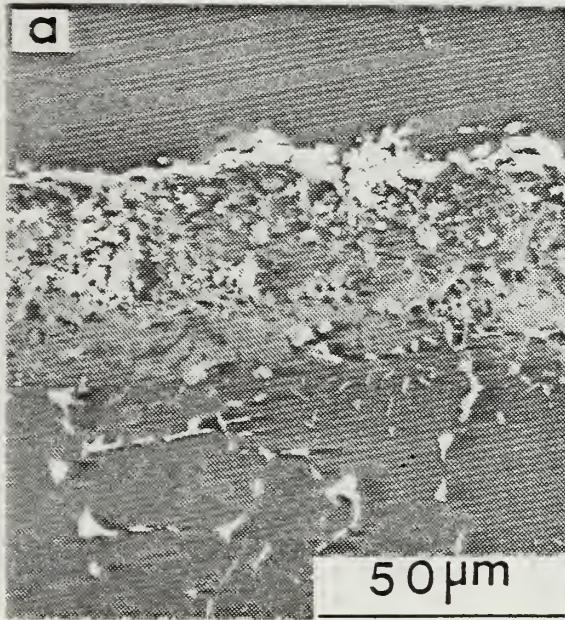


Figure B.15 SEM photomicrographs of CVD-Low Al coatings on MAR-M-509 substrate: (a) exposed 200 hrs at 900 C, (b) exposed 60 hrs at 700 C and (c) as-received.



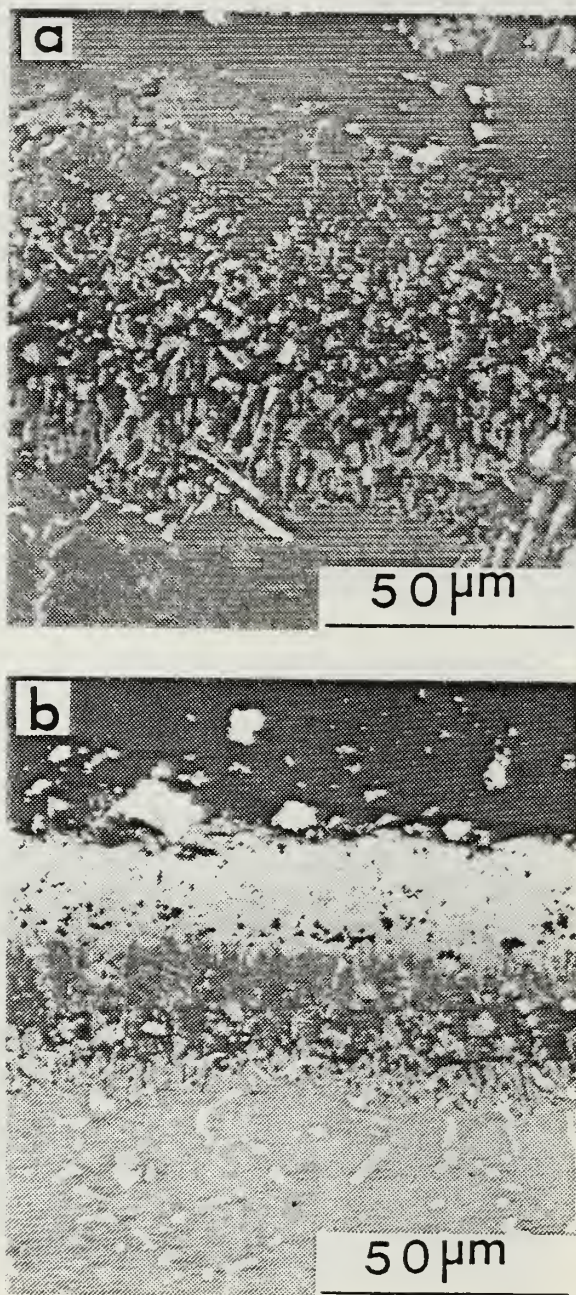


Figure B.16 CEM photomicrographs: (a) Rh-Al coatings and (b) Ph-Pt-Al coatings on MAP-M-509 substrate both exposed 200 hrs at 300 °C.



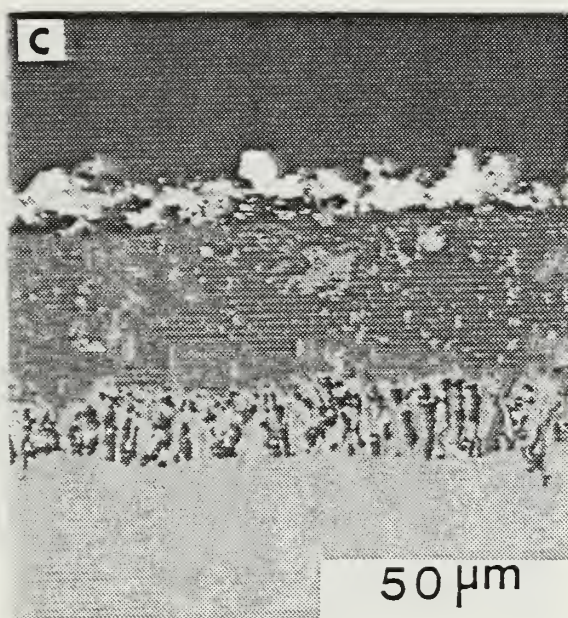
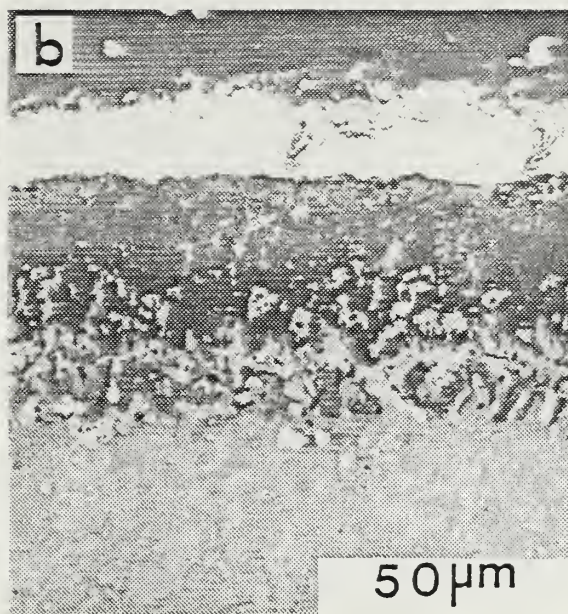
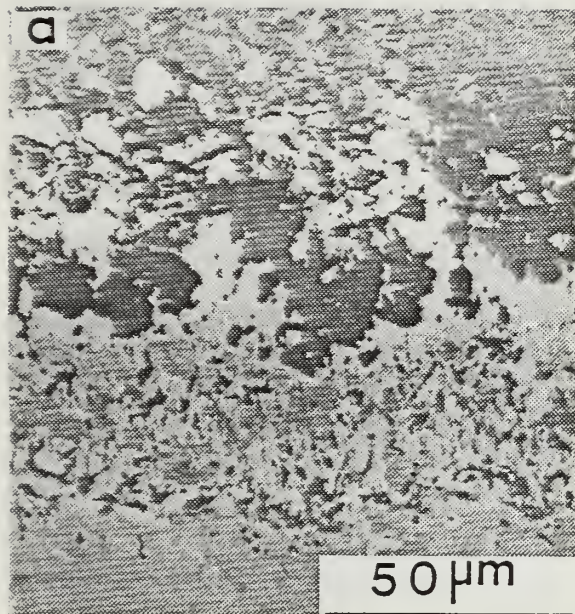


Figure B.17 SEM photomicrographs of Std-Al coatings on K-40 substrate:  
 (a) exposed 200 hrs at 900 °C, (b) exposed 60 hrs at 700 °C and (c) as-received.



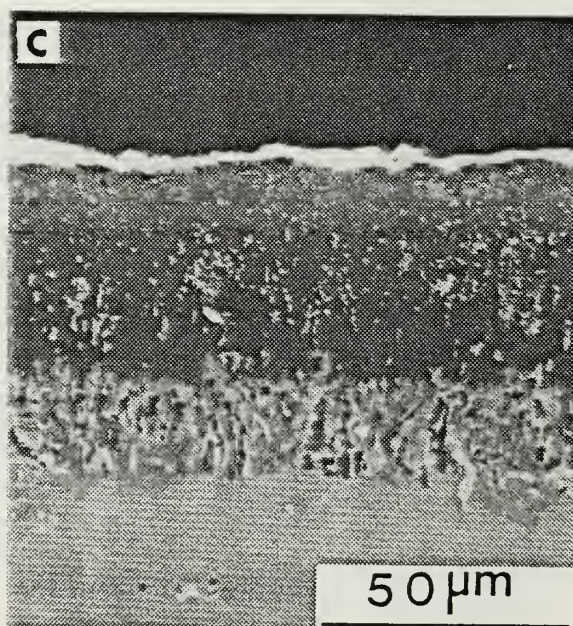
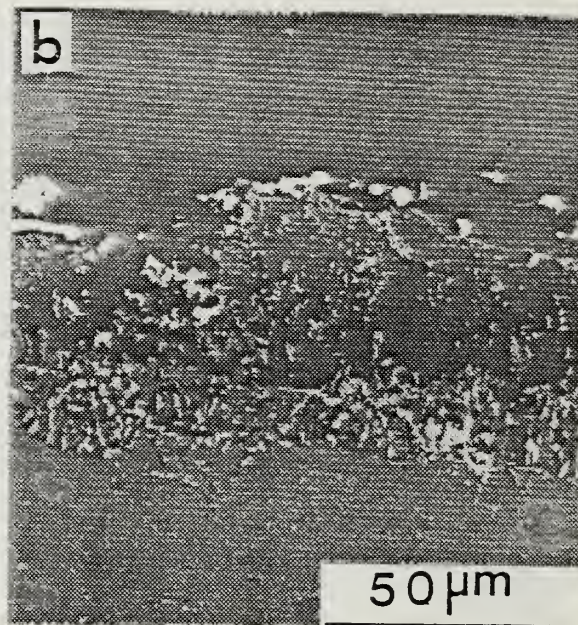
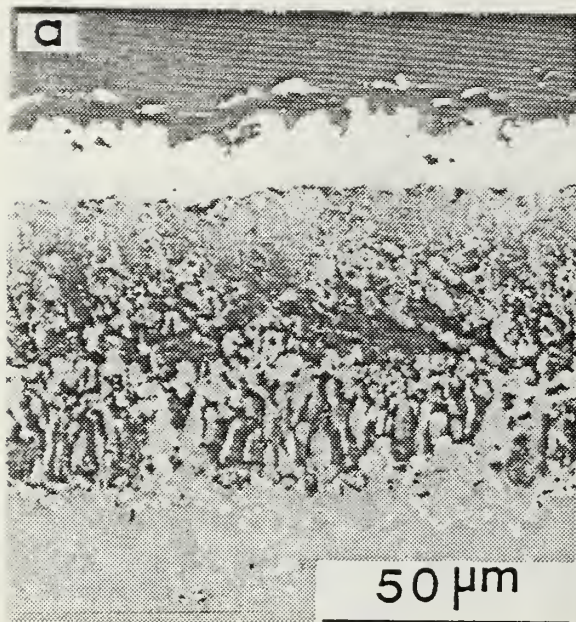


Figure B.18 SEM photomicrographs of Pt-Al coatings on X-40 substrate: (a) exposed 200 hrs at 900 C, (b) exposed 60 hrs at 700 C and (c) as-received.



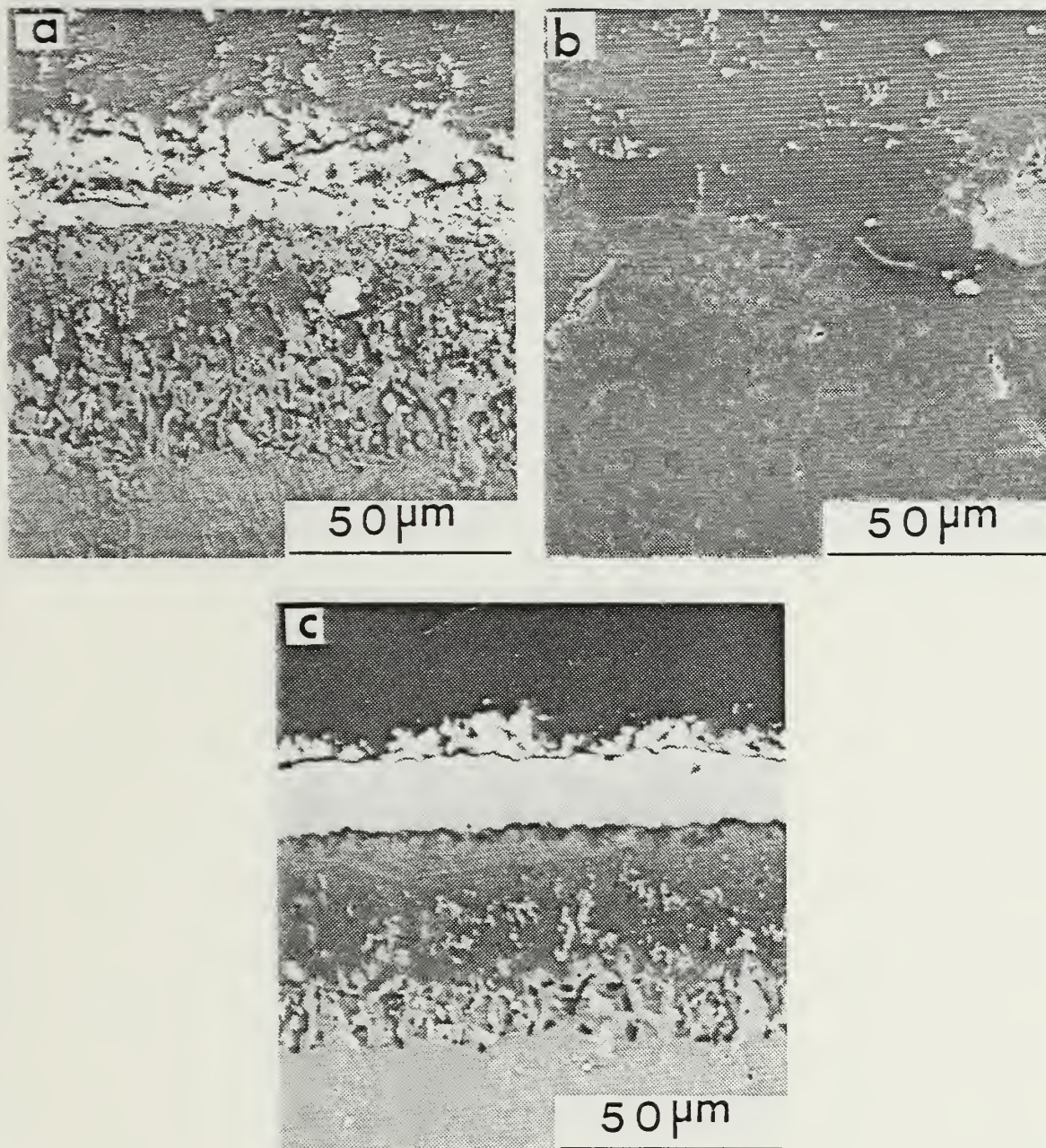


Figure B.19 SEM photomicrographs of Pt-Cr-Al coatings on K-40 substrate: (a) exposed 200 hrs at 900 C, (b) exposed 60 hrs at 700 C and (c) as-received.



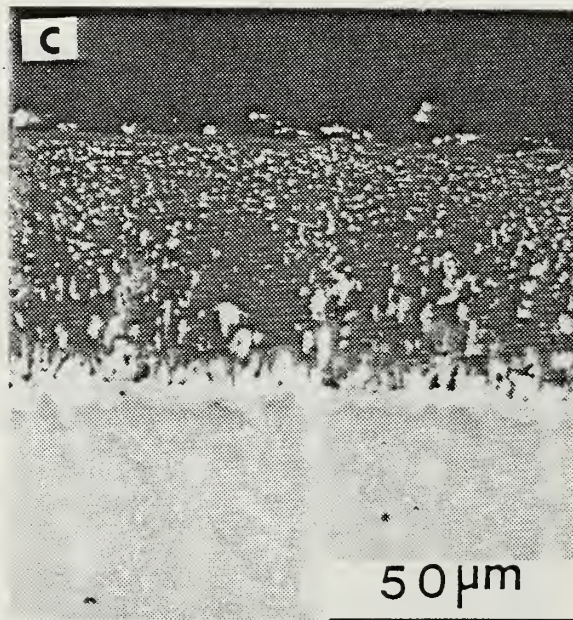
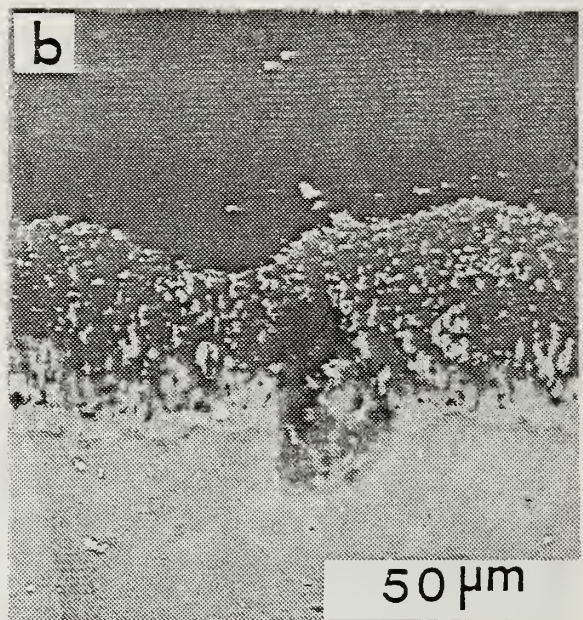
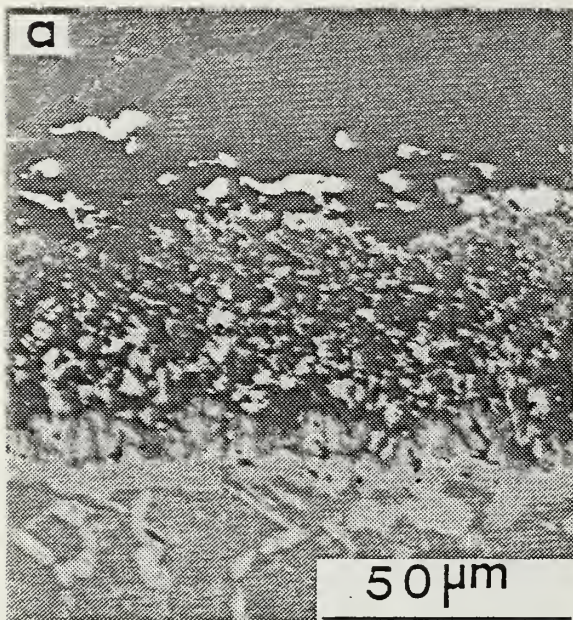


Figure B.20 SEM photomicrographs of Std-Al coatings on FSX-414 substrate: (a) exposed 200 hrs at 900 °C, (b) exposed 60 hrs at 700 °C and (c) as-received.



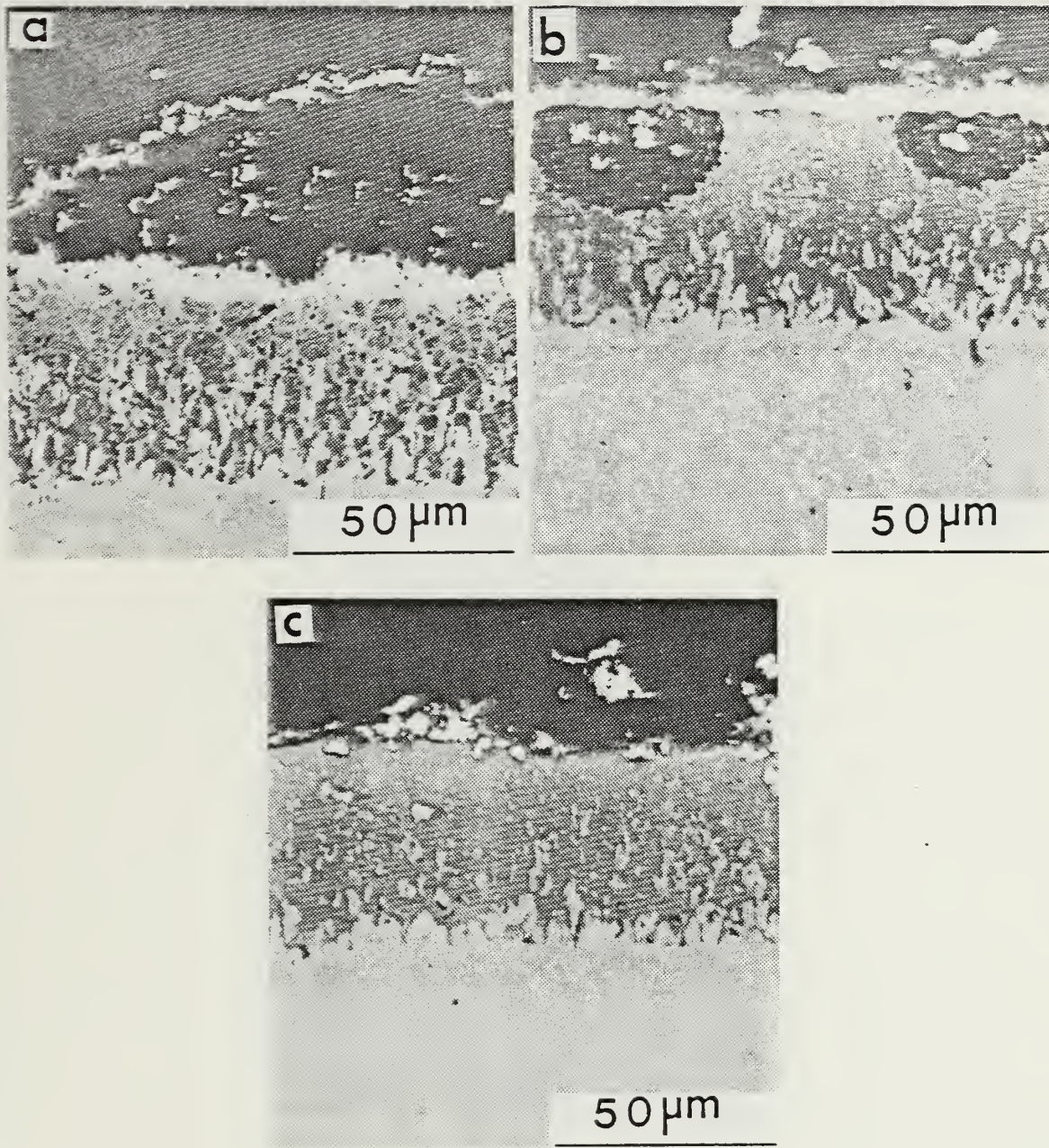


Figure 8.21 SEM photomicrographs of Pt-Al coatings on FSN-414 substrate: (a) exposed 200 hrs at 900 C, (b) exposed 60 hrs at 700 C and (c) as-received.



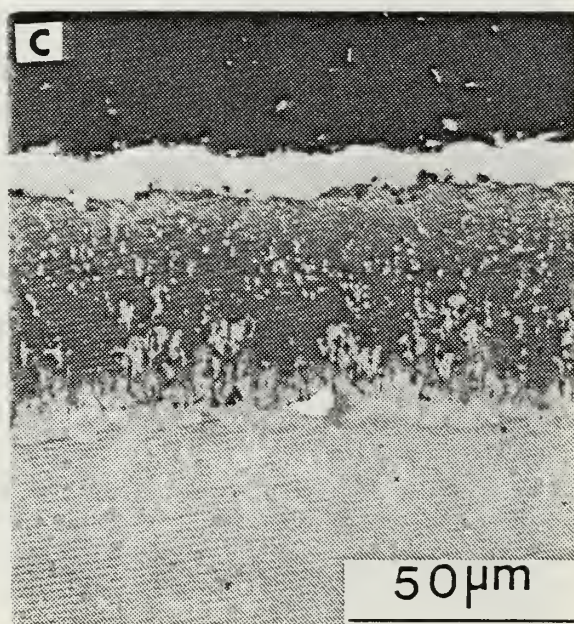
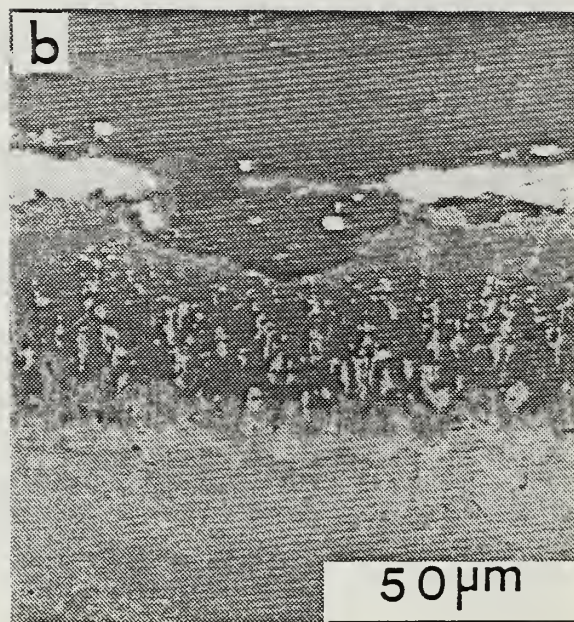
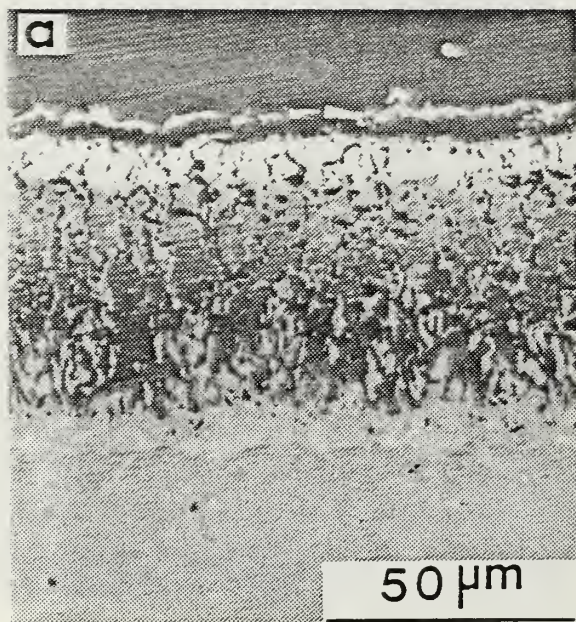


Figure B.22 SEM photomicrographs of Pt-Cr-Al coatings on FCM-414 substrate: (a) exposed 200 hrs at 900 C, (b) exposed 60 hrs at 700 C and (c) as-received.



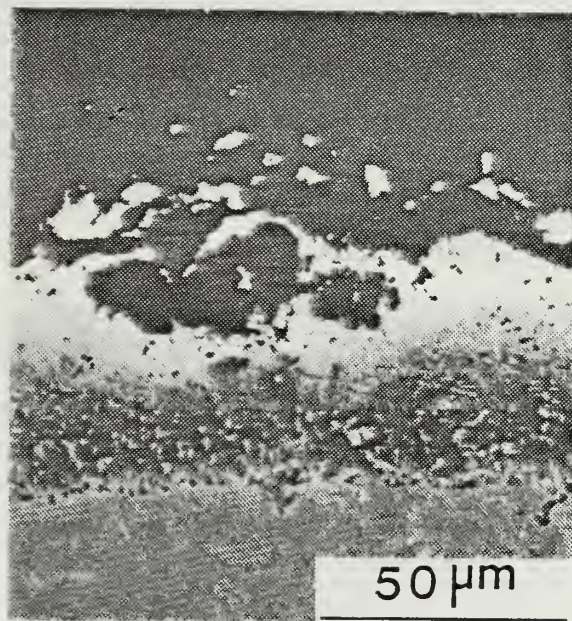


Figure B.23 SEM photomicrographs of Rh-Pt-Al coatings on FSK-414 substrate exposed 200 hrs at 900 C.

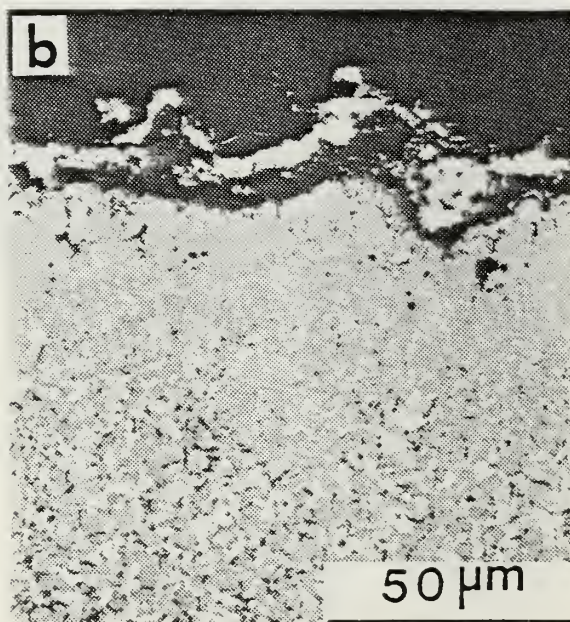
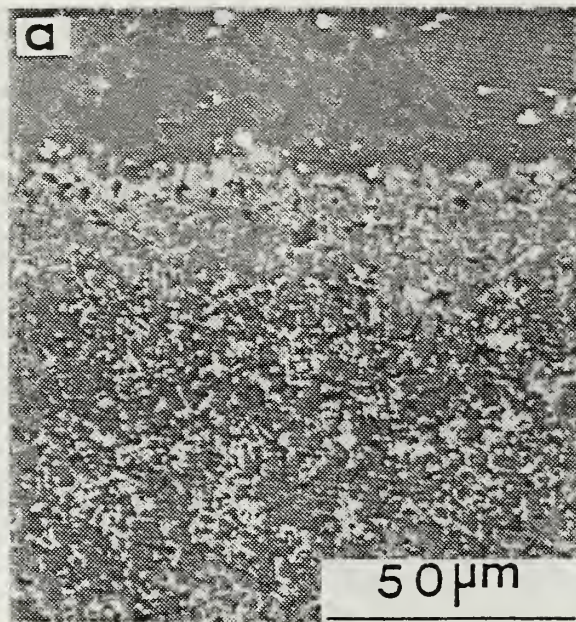


Figure B.24 SEM photomicrographs: (a) aluminide pack process coating and (b) Ph-Al coating on WI-52 substrate both exposed 200 hrs at 900 C.



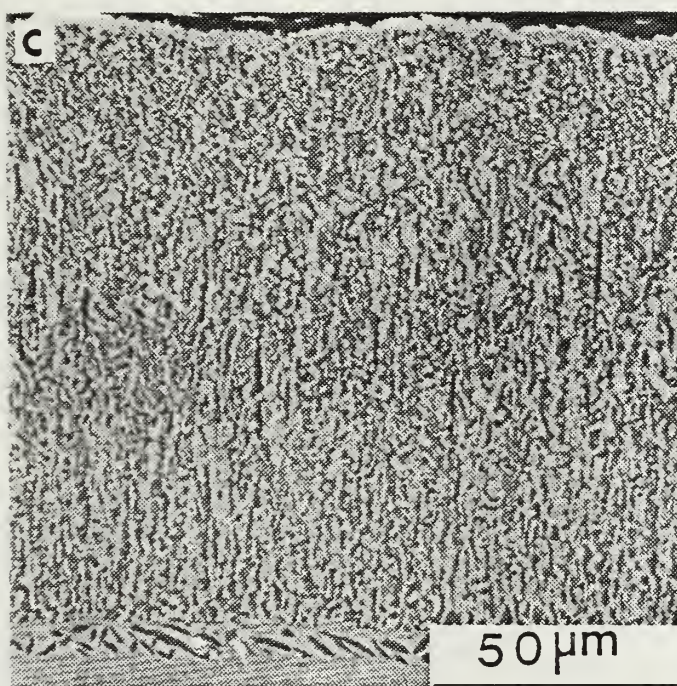
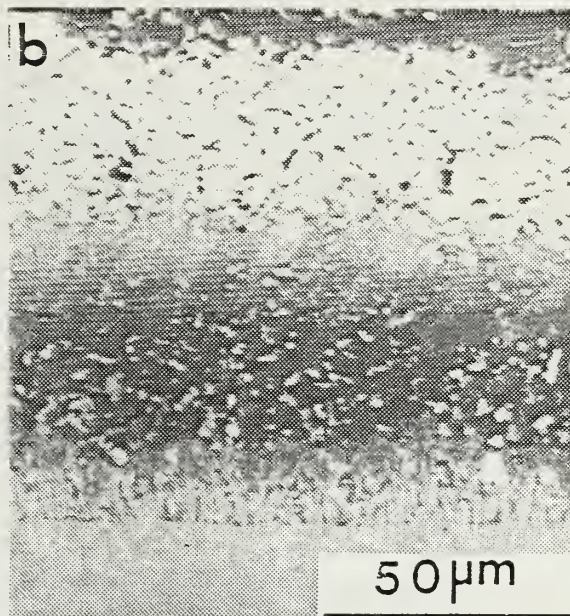
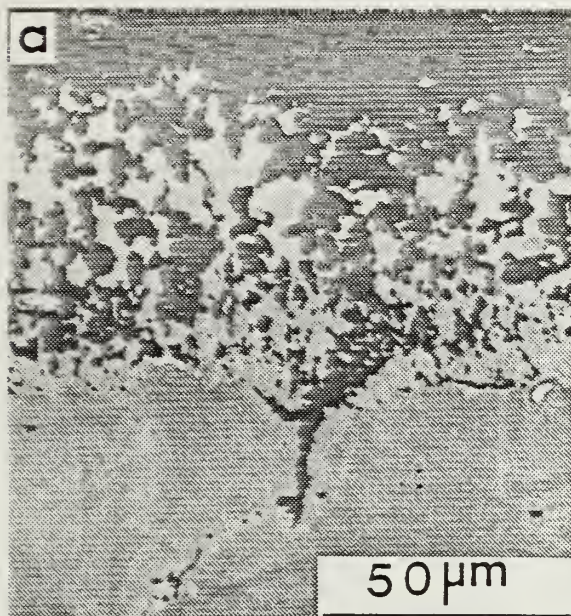


Figure B.25 SEM photomicrographs: (a) EB-PVD CoCrAlY coating exposed 200 hrs at 300 °C, (b) and (c) Pt-Al coatings both exposed 200 hrs at 300 °C and 60 hrs at 700 °C, respectively.

## LIST OF REFERENCES

1. Pyle, E., and Peterson, R., Second Generation Gas Turbines, Naval Engineers Journal, p. 42, August 1969.
2. Shepard, S.B., NAVSEA Marine Gas Turbine Materials Development Program, Naval Engineers Journal, pp. 65-66, August 1981.
3. Pettit, F.S., and Meier, G.H., Oxidation and Hot Corrosion of Superalloys, Superalloys, 1984.
4. Hwang, S.Y., Meier, G.H., Pettit, F.S., Johnston, G.R., Provenzano, Y., and Smidt, F.A., The Initial Stages of Hot Corrosion Attack of CoCrAlY Alloys at 700 C, pp. 121-134 in High Temperature Protective Coating, S.C. Singhal ed., The Metallurgical Society of AIME, Warrendale, PA, 1983.
5. Dust, M.W., Effect of Chromium Addition to the Low Temperature Hot Corrosion Resistance of Platinum Modified Aluminide Coating, Thesis, Naval Postgraduate School, Monterey, California, December 1985.
6. Bornstein, N.S., and DeCrescente, M.A., The Relationship Between Compound of Sodium and Sulfur and Sulfidation, Trans. TMS-AIME, 245, pp. 1947-52, 1969.
7. Goebel, J.A., Pettit, F.S., and Goward, G.W., Mechanisms for the Hot Corrosion of Nickel-Base Alloys, Met. Trans., 4, pp. 261-278, 1973.
8. Fryburg, G.C., Kohl, F.J., and Stearns, C.A., Chemical Reactions Involved in the Initiation of Hot Corrosion of In-738, Published in J. Electrochem. Soc., 1984.



9. Giggins, C.S., and Pettit, F.S., Hot Corrosion Degradation of Metals and Alloys- A Unified Theory, Report prepared by Pratt & Whitney Aircraft, West Palm Beach, Florida, June 1979.
10. Luthra, K.L., and Shore, D.A., Mechanisms of Na SO Induced Corrosion at 600-900 C, J. Electrochem. Soc., 127, pp. 2202-2210, 1980.
11. Luthra, K.L., Low Temperature Hot Corrosion of Cobalt-Base Alloys, part I and part II, Met. Trans. 13A (10), pp. 1943-1952, 1982.
12. Barkalow, R.H., and Pettit, F.S., On the Mechanisms for Hot Corrosion of CoCrAlY Coatings in Marine Gas Turbines, pp. 493-523 in Proceedings of the 4th Conference on Gas Turbine Materials in a Marine Environment, Naval Sea Systems Command, Washington, D.C., June 1979.
13. Hancock, P., The Mechanical Properties of Surface Oxides on Nickel-Base Superalloys - I. Oxidation, Corr. Sci., 18, pp. 527-541, 1978. "The Mechanical Properties of Surface Scales on Nickel-Base Superalloys. II. Contaminant Corrosion," Corr. Sci., 18, pp. 543-553, 1978.
14. Goward, G.W., Protective Coatings for High Temperature Alloys, Proceedings of Symposium on High Temperature Alloys, Electrochem. Soc., Las Vegas, October 1976.
15. Pettit, F.S., and Goward, G.W., High Temperature Corrosion and Use of Coatings for Protection, Metallurgical Treatises, AIME Conference Proceedings, Beijing, China, November 1981.
16. Goward, G.W., Boone, D.H., and Giggins, C.S., Formation and Degradation Mechanisms of Aluminide Coatings on Nickel- Base Superalloys, Transactions ASM, p. 60, 1967.

17. Goward, G.W., and Boone, D.H., Mechanisms of Formation of Diffusion Aluminide on Nickel-Base Superalloys, Oxidation of Metals, vol. 3, no. 5, pp. 475-495, 1971.
18. Paskiet, G.F., Boone, D.H., and Sullivan, C.P., Effects of Aluminide Coating on the High Cycle Fatigue Behavior of a Nickel-Base High Temperature Alloy, J. Inst. Met., 100, 58, 1972 .
19. Vogel, D.J., Determination of the Ductile to Brittle Transition Temperature of Platinum-Aluminide Gas Turbine Blade Coatings, Thesis, Naval Postgraduate School, Monterey, California, September 1985.
20. Svirskii, L.D., Effect of a Thermally Insulated Heat Resistant Coating on the Performance of Gas Turbine Blades, Zhasita Metalov, 6, 733, 1970.
21. Boone, D.H., Peroulakis, A., and Wilkins, C.R., Ceramic-Metal Thermal Barrier Coatings for Gas Turbine Engines, American Ceramic Society, Williamsburg Materials and Applications Forum, September 1974.
22. Singhal, S.C., and Bratton, R.J., Stability of a Zr O (Y O ) Thermal Barrier Coating in Turbine Fuel with Contaminants, Transactions of the ASME, 770, 102, 1980.
23. McKee, D.W., and Siemers, P.A., Resistance of Thermal Barrier Ceramic Coatings to Hot Salt Corrosion, Proceedings of the International Conference on Metallurgical Coatings, p. 439, Elsevier Sequoia S.A., Lausanne and New York, 1980.
24. Hodge, P.E., Miller, R.A., and Gedwill, M.A., Evaluation of the Hot Corrosion Behavior of Thermal Coatings, p. 447, 1980.
25. Goward, G.W., Protective Coatings for High Temperature Gas Turbine Alloys. A Review of the State of Technology, Presented at Les Arcs, NATO, July 1983.



26. Restall, J.E., High Temperature Coatings for Protective Hot Components in Gas Turbine Engines, Metallurgy in Action, pp. 677-682, November 1979.
27. Boone, D.H., Material Coating Techniques, Agard Lecture Series no. 106, paper 8, Lisbon, 1980.
28. Shilling, W.F., Coatings for Heat Engines, Nato Workshop, Aquafredda, 1984.
29. Talboom, F.P.; and Grafwallner, J., Nickel or Cobalt-Base Superalloy with a Coating of Iron, Chromium and Aluminum, U.S. patent 3, 542, 530.
30. Evan, D.J., and Elam, R.C., Cobalt-Base Coating for the Superalloys, U.S. patent 3, 676, 085.
31. Goward, G.W., Boone, D.H., and Pettit, F.S., High Temperature Oxidation Resistant Coating Alloy, U.S. patent 3, 754, 903.
32. Hecht, R.J., Goward, G.W., and Elam, R.C., High Temperature NiCoCrAlY Coatings, U.S. patent 3, 928, 026.
33. Manley II, T.F., Plastic Instability of Aluminide and Platinum Modified Diffusion Coatings During 1100 C Cyclic Testing, Thesis, Naval Postgraduate School, Monterey, California, December 1985.
34. Deb, P., and Boone, D.H., Microstructural Formation and Effects on the Performance of Platinum Modified Aluminide Coatings, Naval Postgraduate School, Monterey, California, November 1985.
35. Lehnert, G., and Meinhardt, H.W., New Protective Coating for Nickel Alloys, Electrodep. Surface Treat. 1, 1972/1973.

36. Streiff, R., Boone, D.H., and Purvis, L.J., Structure of Platinum Modified Aluminide Coatings, NATO Advanced Study Institute, Les Arcs, France, July 1983.
37. Deb, P., Boone, D.H., and Streiff, R., Platinum Aluminide Structural Effects on Hot Corrosion Resistance at 900 C, presented at the 12th ICMC, Los Angeles, California, April 1985, and published in JVSTA, NOV-DEC 1985.
38. Boone, D.H., and Streiff, R., High Temperature Corrosion Resistant Platinum Modified Coatings for Superalloys, presented at the 9th International Congress on Metallic Corrosion, p. 409, Toronto, Canada, 1984.
39. Goward, G.W., Low Temperature Hot Corrosion in Gas Turbines. A Review of Causes and Coatings Thereof, ASME, paper 85-GT-60, p. 3, 1985.
40. Goward, G.W., Protective Coatings - Purpose, Role and Design, Paper presented at the Royal Society Coating Symposium, London, England, pp. 4-5, Nov. 1984.
41. Streiff, R., and Boone, D.H., The Modified Aluminide Coatings Formation Mechanisms of Cr and Pt Modified Coatings, Reactivity of Solids, Elsevier Science Publisher, B.V., Amsterdam, Netherlands, pp. 195-198, 1985.
42. Shankar, S., and Seigle, L.L., Interdiffusion and Intrinsic Diffusion in the NiAl ( $\delta$ ) Phase of the Al-Ni System, Metallurgical transactions, vol. 9A, pp. 1467-1476, Oct. 1978.
43. Dust, M.W., Deb, P., Boone, D.H., and Shankar, S., Hot Corrosion Resistance of Chromium Modified Platinum-Aluminide Coating, to be presented at the June 1986 Gas Turbine Conference, Dusseldorf, W. Germany, and will be published in ASME technical paper.

44. Pettit, F.S., Design of Structural Alloys with High Temperature Corrosion Resistance, pp. 597-621, in Fundamental Aspects of Structural Alloy Design, Jaffee, R.I., and Wilcox, B.A., Plenum Press, New York, 1976.
45. Sims, C.T., and Hagel, W.C., The Superalloys, John Wiley & Son Inc., pp. 318-322, 1972.
46. Shimko, M.J., An Investigation of Substrate Effects on Type Two Hot Corrosion of Marine Gas Turbine Materials, Thesis, Naval Postgraduate School, Monterey, California, June 1983.
47. Aprigliano, L.F., DTNSRDC Report No. DTNSRDC/SME-80/48, p. 6, 1980.
48. Source : Metal Progress Materials and Processing Data Book, pp. 62-67, 1982.
49. Boone, D.H., unpublished work.

# INITIAL DISTRIBUTION LIST

	No.	Copies
1. Defense Technical Information Center Cameron Station Alexandria, Virginia 22304-6145	2	
2. Library, code 0142 Naval Postgraduate School Monterey, California 93943-5000	2	
3. Department Chairman, Code 69Mx Department of Mechanical Engineering Naval Postgraduate School Monterey, California 93943-5000	1	
4. Adjunct Professor D.H. Boone, Code 69B1 Department of Mechanical Engineering Naval Postgraduate School Monterey, California 93943-5000	6	
5. LCDR M. Yasin, Indonesian Navy P.O. Box 47 (C.G.S.C.) Bekasi, Jawa Barat Indonesia	4	







DUDLEY KNOX LIBRARY  
NAVAL POSTGRADUATE SCHOOL  
MONTEREY, CALIFORNIA 95943-8002

219429

Thesis

Y245

c.1

Yasin

Hot corrosion behavior  
of modified aluminide  
coatings on cobalt-base  
superalloys.

219429

Thesis

Y245

c.1

Yasin

Hot corrosion behavior  
of modified aluminide  
coatings on cobalt-base  
superalloys.

thesY245

Hot corrosion behavior of modified alumi



3 2768 000 67755 3

DUDLEY KNOX LIBRARY